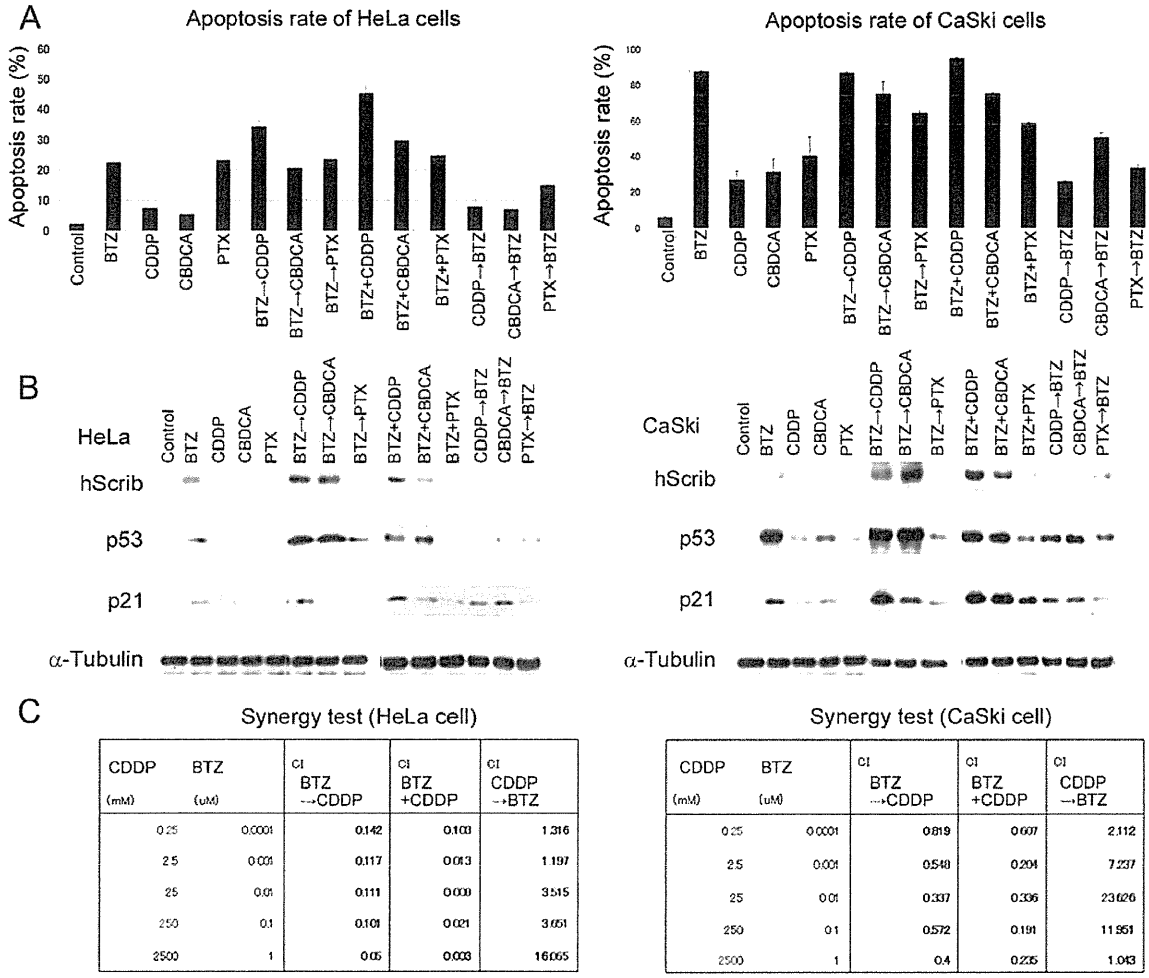

CDDP (mM)	BTZ (uM)	CI BTZ →CDDP	CI BTZ +CDDP	CI CDDP →BTZ
0.25	0.0001	0.142	0.103	1.316
2.5	0.001	0.117	0.013	1.197
25	0.01	0.111	0.009	3.515
250	0.1	0.101	0.021	3.651
2500	1	0.05	0.003	16.065

CDDP (mM)	BTZ (uM)	CI BTZ →CDDP	CI BTZ +CDDP	CI CDDP →BTZ
0.25	0.0001	0.819	0.607	2.112
2.5	0.001	0.548	0.204	7.237
25	0.01	0.337	0.336	23.626
250	0.1	0.572	0.191	11.951
2500	1	0.4	0.235	1.043

Figure 2. An analysis of bortezomib and chemotherapeutic drugs in cervical cancer cells. (A) The rate of apoptosis using bortezomib and chemotherapeutic drugs was measured by flow cytometric analysis. Single, sequential, or simultaneous treatment regimens using bortezomib (100 nM), cisplatin (500 μM), carboplatin (250 μM) or paclitaxel (10 μM) were applied for HeLa and CaSki cells. Bortezomib followed by cisplatin and concomitant bortezomib with cisplatin regimens induced higher apoptosis rates compared with other regimens. Bars represent the means ± SD of 3 independent experiments. (B) Bortezomib stabilized the expression of hScrib and p53 in cervical cancer cell lines in combination with platinum agents. By contrast, cisplatin followed by bortezomib failed to stimulate the expression of hScrib, p53 and p21. (C) Quantification of the potency of the combination treatment. The Chou-Talalay method was utilized. Bortezomib followed by cisplatin and concomitant bortezomib with cisplatin regimens exhibited synergistic effects in all the doses tested. A potent synergistic effect was displayed with CI<0.1. By contrast, a low synergistic or antagonistic effect was shown in the treatment using cisplatin followed by bortezomib with CI>1. BTZ, bortezomib; CDDP, cisplatin; CBDCA, carboplatin; PTX, paclitaxel.

significant treatment regimens in inducing cellular apoptosis (Fig. 2A, lanes 6 and 9) in HeLa cells.

We further investigated the expression of hScrib, p53 and p21, whether the apoptotic effects are indeed associated with protein expressions. Cells were exposed to various concentrations of bortezomib and/or chemotherapeutic drugs (Fig. 2B). The elevated expression of p53 was observed in HeLa cells treated with bortezomib followed by cisplatin or carboplatin (lanes 6 and 7), and in CaSki cells treated with bortezomib alone (lane 2), bortezomib followed by cisplatin or carboplatin (lanes 6 and 7). The expression of hScrib exhibited a similar tendency to that of p53. In terms of the stabilization of p53 and hScrib, paclitaxel turned out to be an unsatisfactory agent (lanes 5, 8, 11 and 14). Markedly, bortezomib and subsequent cisplatin treatment was the most efficient regimen to induce the expression of p21, particularly in CaSki cells (lane 6). Cisplatin followed by bortezomib treatment had an insignificant effect on the expression of p53 and hScrib (lane 12). The apparent recovery of pRb was also observed in HeLa cells treated by the exposure to bortezomib followed by cisplatin (data not shown).

The synergistic effects of bortezomib and cisplatin were analyzed using the Chou-Talalay assay. Bortezomib followed by cisplatin and simultaneous bortezomib with cisplatin regimens were synergistic, with CI<1. This synergy was evidently affected by the order of addition as cisplatin followed by bortezomib showed antagonistic interactions, with CI>1. Therefore, the synergistic effects in HeLa cells was more pronounced compared to that in CaSki cells and we determined to pursue the sequential effect of bortezomib and cisplatin.

In vivo suppression of cervical cancer growth by bortezomib in a mouse xenograft. We analyzed whether bortezomib is able to inhibit tumor growth using a xenograft mouse model of cervical cancer cells. Bortezomib was administered twice a

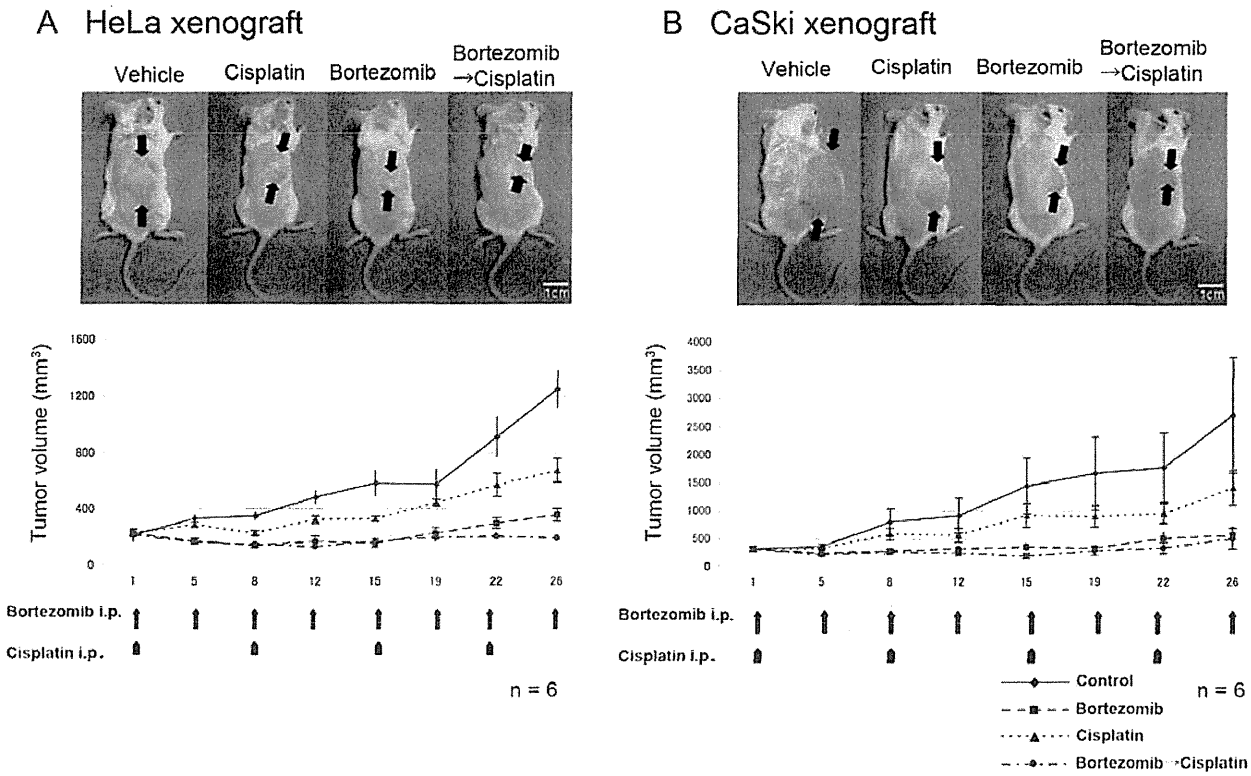

Figure 3. Bortezomib and bortezomib with cisplatin efficiently inhibited the growth of cervical cancer xenografts in athymic mice. (A) Representative images of xenograft mice are shown. Bars indicate 1 cm. (B) HeLa and CaSki cells were transplanted into 6 to 7-week-old athymic mice. When xenograft tumors were visualized, 4 treatment regimens were commenced. Treatment schedules are indicated by thin arrows (bortezomib) and thick arrows (cisplatin). The dose of bortezomib was 1 mg/kg, and the dose of cisplatin was 6 mg/kg, according to the recommendation of the suppliers. Each treatment group consisted of 6 mice. Tumor volumes were calculated as described in Materials and methods. Bars indicate the means ± SEM.

week, and cisplatin once a week according to the instructions of the suppliers. As shown in Fig. 3, the tumor volume of the HeLa and CaSki xenograft was significantly reduced by the injection of bortezomib when compared with the control. The reduction rate of the tumor growth in the bortezomib group was greater than that of cisplatin alone and we revealed that bortezomib with cisplatin was the most efficient treatment regimen in the HeLa xenograft. The CaSki xenograft exhibited a pronounced sensitivity to bortezomib alone and the effect of concomitant use was not observed as expected from the *in vitro* study (Fig. 2, right panel).

Based on the data in Fig. 2, the expression levels of p53, Noxa, and p21 in cervical cancer xenografts were analyzed by western blot analysis. It became evident that p53 and its downstream genes are upregulated in xenografts treated by bortezomib (Fig. 4A and B). Our immunofluorescence study also revealed that the expression of hScrib was recovered at the cellular membrane in mice treated with bortezomib alone or in combination with cisplatin (Fig. 4C and D). The expression of p53 in the nuclei of xenograft cells also increased as a result of treatment of bortezomib (Fig. 4C and D). HeLa and CaSki xenografts were subjected to the detection of apoptosis using TUNEL assay and TUNEL positive cells were observed predominantly in xenograft tumors treated by bortezomib (Fig. 4C and D). These data suggest the possibility that bortezomib inhibits tumor growth *in vivo* through the induction of apoptosis driven by p53 and downstream genes of p53, particularly in HeLa cells.

Discussion

Bortezomib has been shown to be an extremely potent, reversible and selective proteasome inhibitor (26). Several investigators have demonstrated the ability of bortezomib to sensitize a variety of cancer cells to the apoptotic effects of diverse chemotherapeutic agents (12-15,17,27-29). We confirmed that bortezomib was able to induce apoptosis in HPV-positive cervical cancer cell lines. Cisplatin, a critical component of therapeutic regimens in a broad range of malignancies, has been shown to induce apoptosis in various types of cancer cells. For the treatment of advanced or recurrent cervical cancer, cisplatin administered every 3 weeks seems to be a reasonable option, inducing response rates ranging from 20 to 30% and an overall survival of 7 months (30), but prolonged cisplatin treatment appears to have considerable side-effects. We aimed to explore the possibility that concomitant use of bortezomib and chemotherapeutic drugs has additive effects to suppress ubiquitin-mediated degradation of tumor suppressors targeted by E6 in HPV-positive cervical cancer cells both *in vitro* and *in vivo*. As expected, bortezomib alone increased the expression of tumor suppressors such as p53 and hScrib in a dose- and time-dependent manner. We also observed the elevated expression of p21 by the treatment of bortezomib since p21 is a representative downstream gene of p53. We noted that the rate of apoptosis in cells treated with bortezomib preceded by cisplatin was extremely lower than that in cells treated with cisplatin preceded by bortezomib in HeLa cells. The sequential

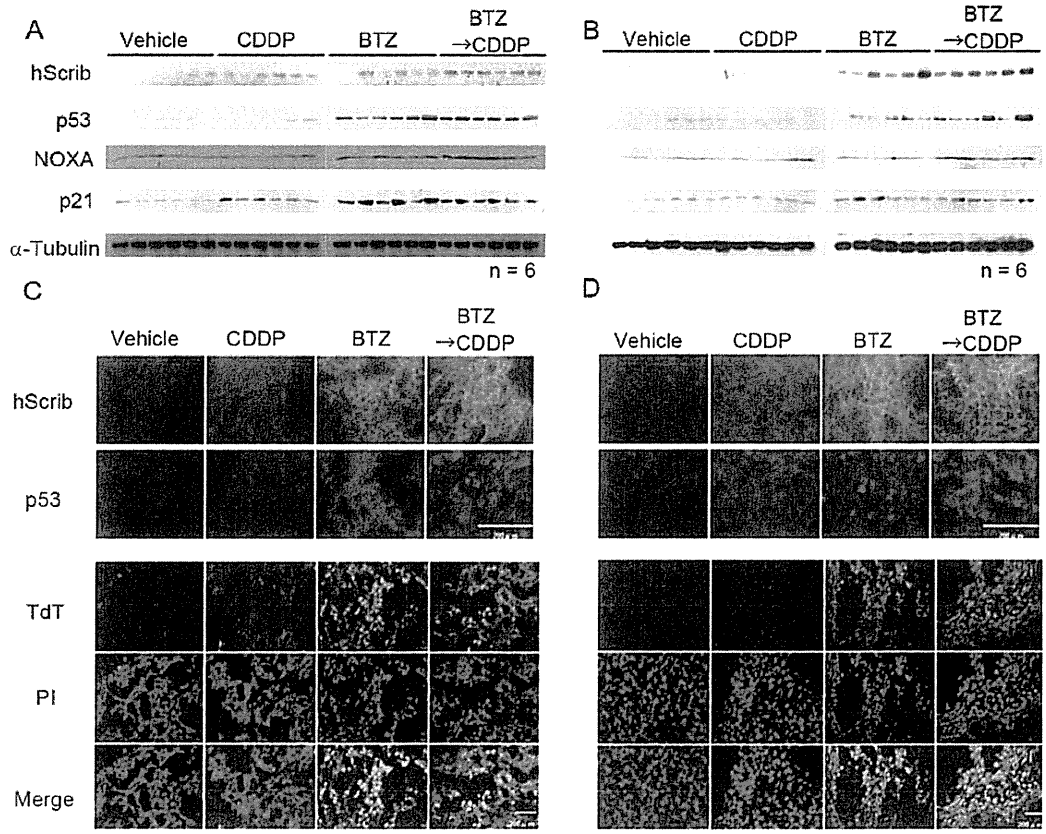

Figure 4. The growth inhibitory effect of bortezomib and cisplatin is evidenced by elevated expression of p53 and hScrib in xenografts of athymic mice. (A and B) Whole cell extracts were obtained from xenograft tumors and the expression levels of hScrib, p53, Noxa and p21 were analyzed by western blotting. (A) HeLa cell xenograft; (B) CaSki cell xenograft. (C and D) The expression levels of hScrib and p53 were visualized by immunofluorescence (upper panel). TUNEL assay revealed that bortezomib and concomitant use of bortezomib and cisplatin induced significant apoptosis in xenograft tumors (lower panel). (C) HeLa cell xenograft; (D) CaSki cell xenograft. Bars indicate 200 μm.

effect (bortezomib followed by cisplatin) on the induction of apoptosis was prominent compared with other combinations. However, this sequential effect was less pronounced in CaSki cells both *in vitro* and *in vivo*, and was similar to a previous report that bortezomib did not induce a sensitization to cisplatin treatment in SiHa cells (16). We must take into account the fact that bortezomib alone was able to induce significant apoptosis in CaSki cells (Fig. 2A, right panel), and this result is in concordance with the result of the Chou-Talalay assay that synergistic effects in HeLa cells were more pronounced compared to those in CaSki cells (Fig. 2C). The optimal sequence of chemotherapies with disparate mechanisms of action has been investigated intensively. Although the mechanisms of the sequence-specific interactions with chemotherapy remain unclear, one possible explanation could be the effect on the apoptotic mechanism by bortezomib. Cisplatin was shown to have a defect in mitochondria-dependent caspase-9 activation in non-small cell lung cancer H460 cells (29). Contrary to this, bortezomib efficiently induced caspase-9 activation and apoptosis by promoting a pro-apoptotic shift in the levels of proteins involved in mitochondrial outer-membrane permeabilization (29). Another mechanism might be its distribution to cell cycle arrest. Bortezomib causes G2/M arrest (31) and cisplatin causes long-lasting blocks at the G1/S boundary with increasing cytotoxicity (32). Theoretically, when bortezomib is administered first, the increased p53 may serve to enhance G1/S checkpoint function. Then G1/S arrest by cisplatin may efficiently enhance apoptotic cell death.

We further examined whether concomitant use of bortezomib and cisplatin can induce apoptosis *in vivo*. Although the regimen was not completely identical to that of the *in vitro* experiment, the concomitant use of bortezomib and cisplatin abrogated the tumor growth of xenografts. In bortezomib-treated tumors, p53 is apparently stabilized in the nuclei of tumor cells, and, subsequently, p21 and Noxa are elevated due to the increased expression of p53. TUNEL assay showed enhanced apoptosis in xenografts treated by bortezomib alone or bortezomib with cisplatin, but concomitant treatment showed significant enhancement of apoptosis. Several investigators have reported the sequence-dependent effects of bortezomib are limited (28,33). The optimal apoptotic effect occurs with the sequence gemcitabine followed by bortezomib in pancreatic cancer cells (33) and in lung cancer cells (28). Therefore, the effect of bortezomib may be sensitization of cancer cells to the apoptotic effect and may be modulating the cellular response to the chemotherapeutics. As a result, bortezomib may enhance cell death in combination with cisplatin. Our data provide new evidence that the schedule of combination treatment must be considered for the treatment of cervical cancer, and gynecologists should consider pre-clinical data in

the design of clinical trials. While it is important to confirm sequential effects in each cancer type studied, it appears that chemotherapy given prior to bortezomib may yield inferior results.

In conclusion, a proteasome inhibitor, bortezomib, induces apoptosis in HPV-positive cervical cancer cells depending on the stabilization of tumor suppressors, particularly p53. When bortezomib is combined with cisplatin, a higher effect of apoptosis induction might be expected since bortezomib plus cisplatin almost completely abolished growth of cervical cancer xenografts with the recovery of p53 and hScrib expression. Our data suggest the possibility that bortezomib plus cisplatin is a promising regimen for the treatment of advanced and/or chemotherapy or radiation therapy-resistant cervical cancer cases.

Acknowledgements

This study was supported by the Mitsui Life Social Welfare Foundation and the grant-in-aid for Scientific Research from the Ministry of Education, Science and Culture, Japan.

References

1. Parkin DM, Bray F, Ferlay J and Pisani P: Global cancer statistics, 2002. CA Cancer J Clin 55: 74-108, 2005.
2. American Cancer Society: Cancer Facts and Figures 2011. http://www.cancer.org/Cancer/CervicalCancer. 2011.
3. Carter JR, Ding Z and Rose BR: HPV infection and cervical disease: a review. Aust N Z J Obstet Gynaecol 51: 103-108, 2011.
4. Berek JS and Hacker NF (eds): Practical Gynaecologic Oncology. 4th edition. Lippincott Williams & Wilkins, Philadelphia, PA, 2005.
5. Nakagawa S, Watanabe S, Yoshikawa H, Taketani Y, Yoshiike K and Kanda T: Mutational analysis of human papillomavirus type 16 E6 protein: transforming function for human cells and degradation of p53 in vitro. Virology 212: 535-542, 1995.
6. Crook T, Tidy JA and Vousden KH: Degradation of p53 can be targeted by HPV E6 sequences distinct from those required for p53 binding and trans-activation. Cell 67: 547-556, 1991.
7. Huibregtse JM and Beaudenon SL: Mechanism of HPV E6 proteins in cellular transformation. Semin Cancer Biol 7: 317-326, 1996.
8. Massimi P, Gammoh N, Thomas M and Banks L: HPV E6 specifically targets different cellular pools of its PDZ domain-containing tumour suppressor substrates for proteasome-mediated degradation. Oncogene 23: 8033-8039, 2004.
9. Nakagawa S and Huibregtse JM: Human scribble (Vartul) is targeted for ubiquitin-mediated degradation by the high-risk papillomavirus E6 proteins and the E6AP ubiquitin-protein ligase. Mol Cell Biol 20: 8244-8253, 2000.
10. Mani A and Gelmann EP: The ubiquitin-proteasome pathway and its role in cancer. J Clin Oncol 23: 4776-4789, 2005.
11. Adams J and Kauffman M: Development of the proteasome inhibitor Velcade (Bortezomib). Cancer Invest 22: 304-311, 2004.
12. Birle DC and Hedley DW: Suppression of the hypoxia-inducible factor-1 response in cervical carcinoma xenografts by proteasome inhibitors. Cancer Res 67: 1735-1743, 2007.
13. Kamer S, Ren Q and Dicker AP: Differential radiation sensitization of human cervical cancer cell lines by the proteasome inhibitor velcade (bortezomib, PS-341). Arch Gynecol Obstet 279: 41-46, 2009.
14. Lin Z, Bazzaro M, Wang MC, Chan KC, Peng S and Roden RB: Combination of proteasome and HDAC inhibitors for uterine cervical cancer treatment. Clin Cancer Res 15: 570-577, 2009.
15. Jiang Y, Wang Y, Su Z, *et al*: Synergistic induction of apoptosis in HeLa cells by the proteasome inhibitor bortezomib and histone deacetylase inhibitor SAHA. Mol Med Rep 3: 613-619, 2010.
16. Bruning A, Vogel M, Mylonas I, Friese K and Burges A: Bortezomib targets the caspase-like proteasome activity in cervical cancer cells, triggering apoptosis that can be enhanced by nelfinavir. Curr Cancer Drug Targets 11: 799-809, 2011.
17. Frankel A, Man S, Elliott P, Adams J and Kerbel RS: Lack of multicellular drug resistance observed in human ovarian and prostate carcinoma treated with the proteasome inhibitor PS-341. Clin Cancer Res 6: 3719-3728, 2000.
18. Nagasaka K, Nakagawa S, Yano T, *et al*: Human homolog of *Drosophila* tumor suppressor Scribble negatively regulates cell-cycle progression from G1 to S phase by localizing at the basolateral membrane in epithelial cells. Cancer Sci 97: 1217-1225, 2006.
19. Morita Y, Wada-Hiraike O, Yano T, *et al*: Resveratrol promotes expression of SIRT1 and StAR in rat ovarian granulosa cells: an implicative role of SIRT1 in the ovary. Reprod Biol Endocrinol 10: 14, 2012.
20. Wada-Hiraike O, Yano T, Nei T, *et al*: The DNA mismatch repair gene hMSH2 is a potent coactivator of oestrogen receptor alpha. Br J Cancer 92: 2286-2291, 2005.
21. Chou TC: Drug combination studies and their synergy quantification using the Chou-Talalay method. Cancer Res 70: 440-446, 2010.
22. Kanai R, Wakimoto H, Martuza RL and Rabkin SD: A novel oncolytic herpes simplex virus that synergizes with phosphoinositide 3-kinase/Akt pathway inhibitors to target glioblastoma stem cells. Clin Cancer Res 17: 3686-3696, 2011.
23. Fraval HN and Roberts JJ: G1 phase Chinese hamster V79-379A cells are inherently more sensitive to platinum bound to their DNA than mid S phase or asynchronously treated cells. Biochem Pharmacol 28: 1575-1580, 1979.
24. Nawrocki ST, Bruns CJ, Harbison MT, *et al*: Effects of the proteasome inhibitor PS-341 on apoptosis and angiogenesis in orthotopic human pancreatic tumor xenografts. Mol Cancer Ther 1: 1243-1253, 2002.
25. Munger K and Howley PM: Human papillomavirus immortalization and transformation functions. Virus Res 89: 213-228, 2002.
26. Adams J: The proteasome: structure, function, and role in the cell. Cancer Treat Rev 29 (Suppl 1): 3-9, 2003.
27. Ling YH, Liebes L, Jiang JD, *et al*: Mechanisms of proteasome inhibitor PS-341-induced G(2)-M-phase arrest and apoptosis in human non-small cell lung cancer cell lines. Clin Cancer Res 9: 1145-1154, 2003.
28. Mortenson MM, Schlieman MG, Virudachalam S and Bold RJ: Effects of the proteasome inhibitor bortezomib alone and in combination with chemotherapy in the A549 non-small-cell lung cancer cell line. Cancer Chemother Pharmacol 54: 343-353, 2004.
29. Voortman J, Checinska A, Giaccone G, Rodriguez JA and Kruyt FA: Bortezomib, but not cisplatin, induces mitochondria-dependent apoptosis accompanied by up-regulation of noxa in the non-small cell lung cancer cell line NCI-H460. Mol Cancer Ther 6: 1046-1053, 2007.
30. Tewari KS and Monk BJ: Gynecologic oncology group trials of chemotherapy for metastatic and recurrent cervical cancer. Curr Oncol Rep 7: 419-434, 2005.
31. Gregory MA and Hann SR: c-Myc proteolysis by the ubiquitin-proteasome pathway: stabilization of c-Myc in Burkitt's lymphoma cells. Mol Cell Biol 20: 2423-2435, 2000.
32. Jackel M and Kopf-Maier P: Influence of cisplatin on cell-cycle progression in xenografted human head and neck carcinomas. Cancer Chemother Pharmacol 27: 464-471, 1991.
33. Fahy BN, Schlieman MG, Virudachalam S and Bold RJ: Schedule-dependent molecular effects of the proteasome inhibitor bortezomib and gemcitabine in pancreatic cancer. J Surg Res 113: 88-95, 2003.

ORIGINAL ARTICLE

The Prevalence of Cervical Regulatory T Cells in HPV-Related Cervical Intraepithelial Neoplasia (CIN) Correlates Inversely with Spontaneous Regression of CIN

Satoko Kojima[1], Kei Kawana[1], Kensuke Tomio[1], Aki Yamashita[1], Ayumi Taguchi[1], Shiho Miura[1], Katsuyuki Adachi[1], Takeshi Nagamatsu[1], Kazunori Nagasaka[1], Yoko Matsumoto[1], Takahide Arimoto[1], Katsutoshi Oda[1], Osamu Wada-Hiraike[1], Tetsu Yano[1], Yuji Taketani[1], Tomoyuki Fujii[1], Danny J. Schust[2], Shiro Kozuma[1]

[1]Department of Obstetrics and Gynecology, Faculty of Medicine, University of Tokyo, Bunkyo-ku, Tokyo, Japan;
[2]Division of Reproductive Endocrinology and Fertility, Department of Obstetrics, Gynecology and Women's Health, University of Missouri School of Medicine, Columbia, MO, USA

Keywords
CD4+CD25+Foxp3+ regulatory T cells, cervical intraepithelial neoplasia, cervical lymphocytes, programmed cell death-1

Correspondence
Kei Kawana, Department of Obstetrics and Gynecology, Faculty of Medicine, University of Tokyo, 7-3-1 Hongo, Bunkyo-ku, Tokyo 113-8655, Japan.
E-mail: kkawana-tky@umin.ac.jp

Submission June 24, 2012;
accepted September 13, 2012.

Citation
Kojima S, Kawana K, Tomio K, Yamashita A, Taguchi A, Miura S, Adachi K, Nagamatsu T, Nagasaka K, Matsumoto Y, Arimoto T, Oda K, Wada-Hiraike O, Yano T, Taketani Y, Fujii T, Schust DJ, Kozuma S. The prevalence of cervical regulatory T cells in HPV-related cervical intraepithelial neoplasia (CIN) correlates inversely with spontaneous regression of CIN. Am J Reprod Immunol 2013; 69: 134–141

doi:10.1111/aji.12030

Problem
Local adaptive cervical regulatory T cells (Tregs) are the most likely direct suppressors of the immune eradication of cervical intraepithelial lesion (CIN). PD-1 expression on T cells induces Tregs. No studies have quantitatively analyzed the Tregs and PD-1+ cells residing in CIN lesions.

Method of study
Cervical lymphocytes were collected using cytobrushes from CIN patients and analyzed by FACS analysis. Comparisons were made between populations of cervical Tregs and PD-1+ CD4+ T cells in CIN regressors and non-regressors.

Results
A median of 11% of cervical CD4+ T cells were Tregs, while a median of 30% were PD-1+ cells. The proportions of cervical CD4+ T cells that were Tregs and/or PD-1+ cells were significantly lower in CIN regressors when compared with non-regressors.

Conclusions
The prevalence of cervical tolerogenic T cells correlates inversely with spontaneous regression of CIN. Cervical Tregs may play an important role in HPV-related neoplastic immunoevasion.

Introduction

HPV infection is a major cause of cervical cancer and its precursor lesion, cervical intraepithelial neoplasia (CIN). Natural history studies of CIN[1,2] show that most infections and most CIN lesions resolve spontaneously; only a minority persists and progress to cervical cancer. Studies showing that HIV-infected women and patients who are under treatment with immunosuppressive agents have an increased incidence of CIN lesions[3,4] suggest that cell-mediated immune response against HPV viral protein is important in the control of HPV infection and progression to CIN. We have previously reported that the presence of gut-derived effector lymphocytes within the cervix plays an important role in local cell-mediated

immune responses and correlates with CIN regression.[5] The presence of robust local tolerogenic cervical T-cell responses to HPV-related neoplastic lesions would be predicted to attenuate the effects of these local effector responses. We hypothesized that the proportion of tolerogenic lymphocytes among the CD4+ T cells in the cervix would decrease among women experiencing CIN regression, thereby allowing full effect of the changes previously seen among local effector cells.

It has been reported that CD4+CD25+Foxp3+ regulatory T cells (Tregs) play an important role in tumor-associated immunoevasion in cancers (ovarian, uterine cervical, endometrial, lung, breast, pancreas, renal cell, and thyroid cancers) as well as in other proliferative disorders such as melanoma and hepatoma.[6–15] Mechanisms underlying Treg suppressive functions have been abundantly reported. The high expression of CD25 (IL-2R) on Tregs has been thought to result in cytokine deprivation-induced apoptosis of effector T cells.[16] IL-10, TGF-β, and IL-35 are also important mediators of Treg suppressive function.[16] Tregs have been reported to suppress T effectors by ligating T-effector-expressed CD80, thereby inhibiting T-cell proliferation and cytokine production. Tregs kill effector T cells, other antigen-presenting cells, and NK cells in a manner dependent on granzyme and perforin.[16]

Natural Treg cells (nTregs) differentiate in the thymus and migrate to peripheral tissues while adaptive/induced Treg cells (iTregs) differentiate in secondary lymphoid organs and tissues including mucosa-associated lymphoid tissues (MALT).[17] iTregs play essential roles in mucosal tolerance, in the control of severe chronic allergic inflammation, in the prevention of parasite and other microorganism clearance, and in the obstruction of tumor immunosurveillance while nTregs have roles in preventing autoimmunity and preventing exaggerated immune responses. iTregs appear in the mesenteric lymph nodes during induction of oral tolerance, differentiate in the lamina propria of the gut in response to microbial signals, and are generated in chronically inflamed tissues. At a minimum, Foxp3+ iTreg development requires TCR stimulation and the cytokines TGF-β and IL-2. Integrin αEβ7+ dendritic cells (DCs) residing in the MALT produce both TGF-β and retinoic acid (RA), which mediate the differentiation of naïve T cells into Foxp3+ iTregs.[17]

The programmed cell death-1 (PD-1) and PD-ligand (PD-L) pathway is also critical in the suppression of immune responses. PD-1 is a molecule inducibly expressed on peripheral CD4+ and CD8+ T cells, NKT cells, B cells, monocytes, and some DC subsets when these cells are activated by antigen receptor signaling and cytokines.[16] nTregs and iTregs can express PD-1 and PD-L1, and the expression of ligand and receptor on the same cell conveys interesting implications. Engagement of PD-1 by its ligands during T-cell receptor (TCR) signaling results in two possible T-cell responses: 1) a diminution in T-effector responses and 2) an augmentation in differentiation of naïve T cells into Foxp3+ iTreg in a TGF-β-dependent manner.[16] There are synergistic effects between the PD-1/PD-L1 pathway and TGF-β in promoting Treg development. PD-L1 is expressed on a wide variety of tumors, and high levels of PD-L1 expression strongly correlate with unfavorable prognosis in a number of cancers.[18] To this point, ligation of PD-1 may induce and maintain iTregs within the tumor microenvironment, enhance the suppression of anti-tumor T-cell responses, and thereby allow tumor progression.

Several previous studies have shown that the prevalence of Tregs among PBMCs increases in CIN patients when compared with healthy controls.[19,20] These studies assess populations of circulating Tregs using flow cytometry. Characterization of the local lymphocytes residing in cervical lesions should better reflect local immune responses to pathogen. While Nakamura et al.[21] used Foxp3 immunostaining of human CIN lesions to report the number of local Foxp3+ cells residing in the CIN lesions by immunostaining of the tissues for Foxp3 and report that the number of Foxp3-immunoreactive cells is higher in CIN3 lesions than normal or CIN1-2 lesions, no studies have quantitatively assessed populations of local Tregs, likely iTregs, in the CIN lesions using flow cytometry. Possible associations between iTregs and the natural course of CIN have also never been studied.

We have previously characterized cervical lymphocytes collected from CIN lesions using a cytobrush and have demonstrated that the majority of cervical lymphocytes in these lesions are CD3+ T cells (median 74%) and that half of the cervical CD3 + T cells are CD4+ (median 54%).[5] In the present investigations, we have analyzed the relative proportions of two tolerogenic T-cell subsets, CD25+Foxp3+ Tregs and PD-1+ T cells, among cervical CD4+ T cells collected from CIN lesions. To determine whether there was a correlation between the frequency of cervical tolerogenic T cell and the natural course of

CIN, comparisons were made between tolerogenic T-cell subsets in the lesions of CIN regressors and non-regressors.

Materials and methods

Study Population

Cervical cell samples were collected using a cytobrush from 24 patients under observation after being diagnosed with CIN by colposcopically directed biopsy. All women gave written informed consent, and the Research Ethics Committee of the University of Tokyo approved all aspects of the study. Patients with known, symptomatic or macroscopically visible vaginal inflammation, or sexually transmitted infections were excluded from our study. To study the association between cervical tolerogenic lymphocytes and CIN progression, CIN patients with regression of cervical cytology (cases) were matched with control patients who did not exhibit cytologic regression over the same time period (measured from initial detection of abnormal cytology). In this study, cytological regression was defined as normal cytology at two or more consecutive evaluations conducted at 3–4 months intervals. For the comparison of CD4+CD25+Foxp3 Tregs and PD1+CD4+ cells, 12 patients were enrolled in the regression group, and the median follow-up duration was 16.5 (8–33) months. Twelve pairs of follow-up time-matched patients with persistent cytological abnormalities were enrolled in the non-regression group, and the median follow-up time was 19 (9–34) months. Patients were interviewed about their smoking history and their last menstrual period.

Collection and Processing of Cervical Lymphocytes

Cervical cells were collected using a Digene cytobrush as described previously.[5] The cytobrush was inserted into the cervical os and rotated several times. The cytobrush was immediately placed in a 15-mL tube containing R10 media (RPMI-1640 medium, supplemented with 10% fetal calf serum, 100 mg/mL streptomycin, and 2.5 μg/mL amphotericin B) and an anticoagulant (0.1 IU/mL of heparin and 8 nM EDTA). After incubating the sample with 5 mM DL-dithiothreitol at 37 °C for 15 min with shaking, the cytobrush was removed. The tube was then centrifuged at 330 *g* for 4 min. The resulting pellet was resuspended in 10 mL of 40% Percoll. This mixture was layered onto 70% Percoll and centrifuged at 480 *g* for 18 min. The mononuclear cells at the Percoll interface were removed and washed with PBS. Cell viability was greater than 95%, as confirmed by trypan blue exclusion, and fresh samples were immediately used for further analyses.

Immunolabeling and Flow Cytometry

Cervical immune cell preparations were immunolabeled with fluorochrome-conjugated mouse monoclonal antibodies specific for the following human leukocyte surface antigens: a programmed death-1 marker (FITC–anti-PD-1), a phycoerythrin cyanine 5.5 (PC5.5)-conjugated helper T-cell marker (PC5.5–anti-CD4), and an allophycocyanin (APC)-conjugated IL-2 receptor marker (APC–anti-CD25). After exposure to primary surface-labeling antibodies, cells were washed twice with FACS buffer (10% fetal calf serum, 1 mM EDTA, 10 mM NaN3), permeabilized with Foxp3 Fixation/Permeabilization working solution (eBioscience, San Diego, CA, USA), and immunolabeled with the anti-intracellular antigen antibody, phycoerythrin (PE)-conjugated anti-Foxp3 marker (PE–anti-Foxp3). Cells were then washed twice with Flow Cytometry Staining Buffer (eBioscience) and resuspended in Flow Cytometry Staining Buffer. Additional aliquots of the cell preparations were labeled in parallel with appropriate isotype control antibodies. Antibodies were purchased from eBioscience and BD (Franklin Lakes, NJ, USA). Data were acquired using four-color flow cytometry on FACSCalibar (Becton-Dickinson, Texarkana, TX, USA). A minimum of 5000 CD4+ T cells was analyzed per sample. The position of CD4+ T cells was determined by CD4 vs SSC gating. We used KALUZA® Flow Analysis Software (Becman Coulter, Brea, CA, USA) for data analysis.

HPV Genotyping

DNA was extracted from cervical smear samples using the DNeasy Blood Mini Kit (Qiagen, Crawley, UK). HPV genotyping was performed using the PGMY-CHUV assay method.[22] Briefly, standard PCR was conducted using the PGMY09/11 L1 consensus primer set and human leukocyte antigen-DQ (HLA-DQ) primer sets. Reverse blotting hybridization was performed. Heat-denatured PCR amplicons were hybridized to specific probes for 32 HPV genotypes

and HLA-DQ reference samples. The virological background (HPV genotyping) of 24 patients in our study is shown in Table I. HPVs 16, 18, 31, 33, 35, 39, 45, 51, 52, 53, 56, 58, 59, 68, 73, and 82 were defined as high-risk HPVs according to an International Agency for Research on Cancer (IARC) multicenter study.[23]

Statistical Analysis

Statistical analyses, including calculation of medians and interquartile ranges (IQRs), were performed using the commercial statistical software package JMP® (SAS, Cary, NC, USA). Wilcoxon rank sum tests or Fisher's exact tests were applied for matched pair comparisons. P-values ≤ 0.05 were considered significant.

Results

Isolation of Cervical Tolerogenic T-cell Subsets in CIN Lesions

To assess cervical tolerogenic T cells, cervical samples were collected from CIN lesions positive for any HPV genotype and fractionated over a discontinuous Percoll density gradient to remove cervical epithelial cells. Cervical lymphocytes were then isolated from the interphase between Percoll and culture medium.[5] Cervical CD4+ T cells were identified among the isolated lymphocytes using CD4 vs SSC gating. The percentages of CD4+ cervical T cells that were CD25+Foxp3+ Tregs or that were PD-1+ were determined by flow cytometry. Two representative cases are displayed in Fig. 1(a,b), respectively. The proportion of cervical CD4+ T cells that were CD25+Foxp3+ was 14.2% whereas the proportion of CD4+ T cells that displayed PD-1 was 33.6% (bold lines). Among all CIN patients, a median of 11.7% (IQR: 7.3–14.6, $n = 24$) of CD4+ cervical T cells were CD25+Foxp3+ Tregs, while a median of 30.7% (20.2–38.5, $n = 24$) of CD4+ cells expressed PD-1. The proportions of tolerogenic T-cell subsets found in cervical preparations were markedly higher than those reported in circulating peripheral blood where approximately 5% of PBMCs are CD25+Foxp3+ Tregs[24] and 5% of peripheral CD4+ T cells are PD-1+.[25] These data indicate that the cervical mucosal T cells separation technique used for these investigations isolated a population of T cells with characteristics that suggest little to no contamination by peripheral blood. Further, should small amounts of contamination occur during isolation the effect on overall results would be predicted to be minimal.

Table I Patients infected with multiple HPV types were included.

HPV type	Total numbers (%)
16	5 (16.6)
18	2 (6.6)
31	1 (3.3)
45	1 (3.3)
51	1 (3.3)
52	3 (10)
53	3 (10)
55	3 (10)
56	4 (13.3)
58	5 (16.6)
70	2 (6.6)
Total	30 (100)

Of 24 patients, 4 (16.6%) were infected with multiple types. HPVs 16, 18, 31, 33, 35, 39, 45, 51, 52, 53, 56, 58, 59, 68, 73, and 82 were defined as high-risk HPVs.

Correlation of Cervical Tregs and PD-1+ CD4+ cells in CIN Lesions with Menstrual Phase, HPV Types, Smoking History, and CIN Course

Many factors, including HPV genotypes, smoking, and other microbial infections, have been reported to associate with spontaneous regression or progression of CIN.[26] In this study, we obtained cervical Tregs from histologically diagnosed CIN patients and sought correlations between cervical Tregs and potential clinical factors, which may associate with the natural course of CIN. Patients with known, symptomatic or macroscopically visible vaginal inflammation, or sexually transmitted infections other than HPV were excluded from our study. All patients were diagnosed with CIN1-2 at the time of enrollment and followed with colposcopy and cervical cytology smears every 4 months.

To account for possible confounding factors, samples from our 24 CIN patients were reanalyzed after segregation by each of the following characteristics: menstrual phase (proliferative vs secretory), HPV genotype (high risk vs low risk), and smoking history (smoking vs non-smoking). The prevalence of CD25+Foxp3+ Tregs and of PD-1+ T cells among cervical CD4+ cells was compared between each of the

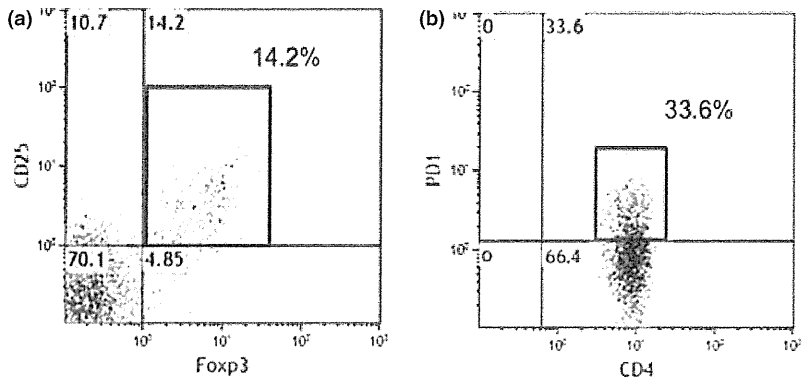

Fig. 1 Representatives of flow cytometric analysis of immune cells isolated from cervical intraepithelial neoplasia lesions. Bold lines delimit cervical CD4+CD25+Foxp3+ Tregs (a) and PD1+ CD4+ T cells (b). The indicated percentages represent percentage of total CD4+ T cells.

two groups using Wilcoxon rank sum testing (Table II). None of these possible confounders correlated with CD25+Foxp3+ Tregs and PD-1+ T cells results in CIN lesions, indicating that the tolerogenic T cells residing in the cervical mucosa were not influenced by smoking, hormonal status, or infecting HPV subtypes.

Next, we compared populations of CD25+Foxp3+ Tregs and PD-1+ T cells residing in the CIN lesions of regressors (n = 12) and non-regressors (n = 12) to determine whether there was an association between the frequency of cervical tolerogenic T-cell subsets and spontaneous regression of CIN. Twelve patients had spontaneous regression of their CIN lesions, and these women had a median follow-up duration of 16.5 (8–33) months. The non-regression group consisted of twelve women with persistent cytological abnormalities who were matched to the spontaneous regressor cohort by follow-up time. No significant differences were seen in the detection rates of high-risk HPV (58.3% vs 83.3%, P = 0.37), percent of CIN 2 at the enrollment (33.3% vs 58.3%, P = 0.4), and the median ages (33 years old vs 36, P = 0.44) of patients in the regression and non-regression groups. Among regressors, cervical CD25+Foxp3+ Tregs comprised a median of 7.3% (IQR: 6.3–11.4) of cervical CD4+ cells; the rate among non-regressors was 13.9% (IQR: 11.6–16.9). The frequency of cervical CD25+Foxp3+ Tregs in regressors was significantly lower than that in non-regressors (P = 0.0012) (Table II and Fig. 2). Similarly, cervical PD1+ CD4+ cells comprised a median of 20.8% (IQR: 15.8–31.9) of cervical CD4+ cells among regressors whereas a median of 35.1% (IQR:

Table II Correlation of the proportions of cervical Treg and PD-1+ cells among cervical CD4+ T-cell populations with clinical characteristics

		Percentage of total cervical CD4+ T cells			
Factors	Groups	CD25+Foxp3+ Tregs		PD-1+ cells	
Menstrual phase	Proliferative	10.26 (7.04–15.4)	P = 0.94	29.8 (22.7–39.5)	P = 0.72
	Secretory	12.0 (7.1–14.2)		28.1 (18.9–36.7)	
HPV genotype	High risk	11.8 (7.8–14.2)	P = 0.67	29.8 (20.3–38.2)	P = 0.82
	Low risk	7.4 (6.7–15.7)		33.5 (18.5–45.4)	
Smoking	Smoking	10.2 (7.3–14.7)	P = 0.73	29.8 (19.5–39.5)	P = 0.80
	Non-smoking	10.8 (5.0–15.9)		24.6 (19.6–40.9)	
CIN course	Regression	7.3 (6.3–11.4)	P = 0.0012	20.8 (15.8–31.9)	P = 0.018
	Non-regression	13.9 (11.6–16.9)		35.1 (30.2–42.6)	

Association of cervical CD4+CD25+Foxp3+ Tregs and PD1+CD4+ cells with menstrual cycle, HPV genotype, smoking, and cervical intraepithelial neoplasia (CIN) course were shown.

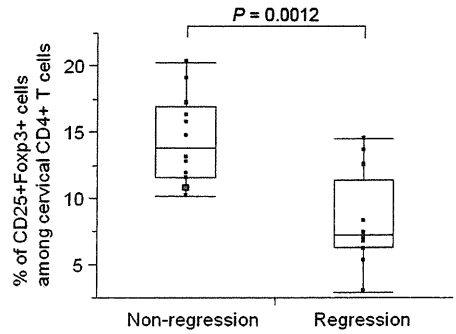

Fig. 2 Association of cervical Tregs with the natural course of cervical intraepithelial neoplasia. Among regressors, cervical Tregs comprised a median of 7.33% [Interquartile ranges (IQR): 6.38–11.4, n = 12] of CD4+ cervical T cells; the rate among non-regressors was 13.9% (IQR: 11.6–16.9, n = 12); P = 0.0012.

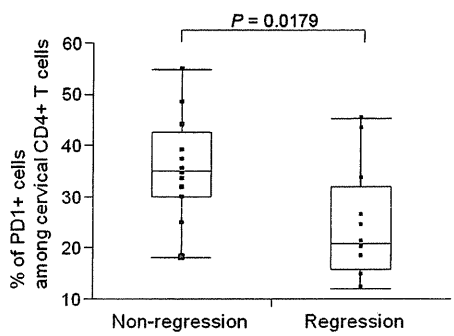

Fig. 3 Association of cervical PD-1+ CD4+ T cells with the natural course of cervical intraepithelial neoplasia. Among regressors, cervical PD1+ cells comprised a median of 20.8% [Interquartile ranges (IQR): 15.8–31.9, n = 12] of CD4+ cervical T cells; the rate among non-regressors was 35.1% (IQR: 30.2–42.6, n = 12); P = 0.0179.

30.2–42.6) among non-regressors. Again, the frequency of cervical PD-1+ CD4+ cells in regressors was significantly lower than that in non-regressors (P = 0.017) (Table II and Fig. 3).

Discussion

Although many studies have been reported about the positive association between tolerogenic lymphocytes and poor prognosis in many cancers, there are limited data on similar associations in women with HPV-related cervical precursor lesions. Our results show that the prevalence of CD25+ Foxp3+ Tregs and of PD1+ CD4+ T cells residing in cervical precursor lesions inversely correlates with spontaneous regression of CIN.

The peripheral population of Foxp3+ Tregs includes nTregs and iTregs. iTregs play essential roles in mucosal tolerance, in the control of severe chronic allergic inflammation, and in the prevention of organism clearance and tumor immunosurveillance, while nTregs have roles in preventing autoimmunity and exaggerated immune responses.[17] We would predict that the majority of cervical CD25+Foxp3+ Tregs assessed in this study are iTregs although definitive isolation of iTregs is hampered by the lack of suitable surface markers that distinguish iTreg and nTreg cell populations.

In this study, cervical Treg prevalence negatively correlated with regression of CIN (Fig. 2) but did not correlate with CIN grade (data not shown). Supporting our data, several previous studies have shown a positive correlation between Treg prevalence in peripheral blood and high grade of CIN.[19,20] Of course, cervical iTregs and circulating Tregs may differ in their TCR repertoire. iTregs are known to differentiate from mature naïve CD4+ cells through the effects of TGF-β and RA secreted by mucosa-associated DCs.[17] In our data, the proportion of CD25+Foxp3+ Tregs among total cervical CD4+ cells (a median of 11%) was twofold higher than previously reported peripheral blood levels (approximately 5%). This suggests that iTregs may be generated continuously, probably in an antigen-depending manner, and accumulate in chronically HPV-infected tissues and CIN lesions. Others have reported that Foxp3 mRNA levels in cervical samples that included exfoliated epithelial cells and cervical lymphocytes are higher among high-grade squamous intraepithelial lesion (HSIL) patients when compared with low-grade squamous intraepithelial lesion (LSIL) patients.[27] However, it is unknown whether Foxp3 mRNA levels in these cervical samples parallel the number of Tregs because cervical lymphocytes were not specifically isolated in this study.

Although the persistence of HPV infection was not followed in the present study, Molling et al.[20] reported that CD4+CD25hi Treg frequency correlates with persistence of HPV type 16. Tregs may inhibit the HPV clearance by immune cells such as invariant natural killer T cells.

TGF-β is critical to the induction and maintenance of Foxp3+ Tregs, with particular importance in the induction of iTregs from naive T cells and in the conversion of effector T cells to iTregs. Several studies have demonstrated that the expression of TGF-β and RA receptors in cervical specimens is lower in

CIN lesions when compared with normal epithelium.[28,29] In these studies, there was no correlation between TGF-β mRNA levels and either CIN grade or CIN natural course. TGF-β-induced iTreg frequency may be a more direct predictor of CIN progression than TGF-β. In fact, measurement of tolerogenic T-cell frequency in CIN lesions has the potential to prove useful in determining individualized screening and treatment paradigms.

Whether sex hormones modulate the prevalence and function of Tregs remains controversial. Arruvito et al. reported that the proportion of Foxp3+ cells within the peripheral blood CD4+ T-cell population increases during the late follicular phase when compared with the luteal phase.[29] The expansion of Tregs during the follicular phase was highly correlated with serum estradiol (E2) levels.[30] In contrast, Weinberg et al. reported recently that there are no significant correlations between changes in serum E2 levels and the prevalence of any circulating Treg subtypes or between changes in serum progesterone levels and the proportion of CD8+ Foxp3+ Tregs in peripheral blood samples.[31] The effect of smoking on the generation of tolerogenic T cells is also controversial.[32–34] Note that all of the above studies assess peripheral circulating rather than local cervical Tregs. Our data on the latter cells revealed no correlations between cervical Treg prevalence and either menstrual phase or smoking.

In this study, we focused on PD-1+ CD4+ T cells as well as Foxp3+ Tregs as engagement of PD-1 by its ligands on T cells is critical to the differentiation of naïve T cell into Foxp3+ iTregs. Furthermore, Tregs and the PD-1/PD-L pathway are integral in terminating immune responses and augmenting the suppression of anti-tumor T-cell responses. In short, the PD-1 pathway controls the development, maintenance, and function of iTregs at mucosal sites. Here, we show that PD-1+ T cells are more frequently found among cervical T cells than among PBMCs and that the prevalence of PD1+ T cells in CIN lesions (likely reflecting cervical iTregs) correlates inversely with spontaneous regression of CIN. Assessment for other tolerogenic T-cell subsets (e.g., Foxp3-IL10+ Tr1, Foxp3-TGF-β+ Th3) in this study, while potentially informative, was limited by the number of cervical lymphocytes that could be isolated from a single cytobrush sample.

In summary, even the study population is small and the results are limited, our flow cytometric analyses demonstrate for the first time that a prevalence of CD4+ CD25+ Foxp3+ Tregs infiltrating into CIN lesions significantly correlates with regression of CIN regardless of HPV subtype. Conversely, a high prevalence of lesional cervical Tregs may be responsible for CIN persistence as well as HPV infections and might function as a useful predictive biomarker for progression of CIN.

Acknowledgements

We thank Dr. Ai Tachikawa-Kawana for expert advice about flow cytometry. This work was supported by a grant from the Ministry of Health, Labour and Welfare of Japan for the Third-Term Comprehensive Strategy for Cancer Control and for Comprehensive Strategy for Practical Medical Technology and by a grant from the Ministry of Education, Culture, Sports, Science and Technology of Japan and by a grant from Tokyo IGAKUKAI.

References

1 Holowaty P, Miller AB, Rohan T, To T: Natural history of dysplasia of the uterine cervix. *J Natl Cancer Inst* 1999; 91:252–258.
2 Moscicki AB, Schiffman M, Kjaer S, Villa LL: Chapter 5: updating the natural history of HPV and anogenital cancer. *Vaccine* 2006; 24:42–51.
3 Ellerbrock TV, Chiasson MA, Bush TJ, Sun XW, Sawo D, Brudney K, Wright TC Jr: Incidence of cervical squamous intraepithelial lesions in HIV-infected women. *JAMA* 2000; 283:1031–1037.
4 Ognenovski VM, Marder W, Somers EC, Johnston CM, Farrehi JG, Selvaggi SM, McCune WJ: Increased incidence of cervical intraepithelial neoplasia in women with systemic lupus erythematosus treated with intravenous cyclophosphamide. *J Rheumatol* 2004; 31:1763–1767.
5 Kojima S, Kawanna K, Fujii T, Yokoyama T, Miura S, Tomio K, Tomio A, Yamashita A, Adachi K, Sato H, Nagamatsu T, Schust DJ, Kozuma S, Taketani Y: Characterization of Gut-Derived Intraepithelial Lymphocyte (IEL) Residing in Human Papillomavirus (HPV)-Infected Intraepithelial Neoplastic Lesions. *Am J Reprod Immunol* 2011; 66:435–443.
6 Wolf D, Wolf AM, Rumpold H, Fiegl H, Zeimet AG, Muller-Holzner E, Deibl M, Gastl G, Gunsilius E, Marth C: The expression of the regulatory T cell-specific forkhead box transcription factor FoxP3 is associated with poor prognosis in ovarian cancer. *Clin Cancer Res* 2005; 11:8326–8331.
7 Jordanova ES, Gorter A, Ayachi O, Prins F, Durrant LG, Kenter GG, van der Burg SH, Fleuren GJ: Human leukocyte antigen class I, MHC class I chain-related molecule A, and CD8+/regulatory T-cell ratio: which variable determines survival of cervical cancer patients? *Clin Cancer Res* 2008; 14:2028–2035.
8 Yamagami W, Susumu N, Tanaka H, Hirasawa A, Banno K, Suzuki N, Tsuda H, Tsukazaki K, Aoki D: Immunofluorescence-detected infiltration of CD4+FOXP3+ regulatory T cells is relevant to the prognosis of patients with endometrial cancer. *Int J Gynecol Cancer* 2011; 21:1628–1634.

9 Koyama K, Kagamu H, Miura S, Hiura T, Miyabayashi T, Itoh R, Kuriyama H, Tanaka H, Tanaka J, Yoshizawa H, Nakata K, Gejyo F: Reciprocal CD4+ T-cell balance of effector CD62Llow CD4+ and CD62LhighCD25+ CD4+ regulatory T cells in small cell lung cancer reflects disease stage. *Clin Cancer Res* 2008; 14:6770–6779.

10 Liu F, Lang R, Zhao J, Zhang X, Pringle GA, Fan Y, Yin D, Gu F, Yao Z, Fu L: CD8 cytotoxic T cell and FOXP3 regulatory T cell infiltration in relation to breast cancer survival and molecular subtypes. *Breast Cancer Res Treat* 2011; 130:645–655.

11 Yamamoto T, Yanagimoto H, Satoi S, Toyokawa H, Hirooka S, Yamaki S, Yui R, Yamao J, Kim S, Kwon AH: Circulating CD4 +CD25+ regulatory T cells in patients with pancreatic cancer. *Pancreas* 2012; 41:409–415.

12 Jacobs JF, Nierkens S, Figdor CG, de Vries IJ, Adema GJ: Regulatory T cells in melanoma: the final hurdle towards effective immunotherapy? *Lancet Oncol* 2012; 13:32–42.

13 Liotta F, Gacci M, Frosali F, Querci V, Vittori G, Lapini A, Santarlasci V, Serni S, Cosmi L, Maggi L, Angeli R, Mazzinghi B, Romagnani P, Maggi E, Carini M, Romagnani S, Annunziato F: Frequency of regulatory T cells in peripheral blood and in tumour-infiltrating lymphocytes correlates with poor prognosis in renal cell carcinoma. *BJU Int*, 2011; 107:1500–1506.

14 Fu J, Xu D, Liu Z, Shi M, Zhao P, Fu B, Zhang Z, Yang H, Zhang H, Zhou C, Yao J, Jin L, Wang H, Yang Y, Fu YX, Wang FS: Increased regulatory T cells correlate with CD8 T-cell impairment and poor survival in hepatocellular carcinoma patients. *Gastroenterology* 2007; 132:2328–2339.

15 French JD, Weber ZJ, Fretwell DL, Said S, Klopper JP, Haugen BR: Tumor-associated lymphocytes and increased FoxP3+ regulatory T cell frequency correlate with more aggressive papillary thyroid cancer. *J Clin Endocrinol Metab* 2010; 95:2325–2333.

16 Francisco LM, Sage PT, Sharpe AH: The PD-1 pathway in tolerance and autoimmunity. *Immunol Rev* 2010; 236:219–242.

17 Maria A, Lafaille C, Lafaille JJ: Natural and adaptive Foxp3+ regulatory T cells: more of the same or a division of labor? *Immunity* 2009; 30:626–635.

18 Driessens G, Kline J, Gajewski TF: Costimulatory and coinhibitory receptors in anti-tumor immunity. *Immunol Rev* 2009; 229:126–144.

19 Visser J, Nijman HW, Hoogenboom BN, Jager P, van Baarle D, Schuuring E, Abdulahad W, Miedema F, van der Zee AG, Daemen T: Frequencies and role of regulatory T cells in patients with (pre) malignant cervical neoplasia. *Clin Exp Immunol* 2007; 150:199–209.

20 Molling JW, de Gruijl TD, Glim J, Moreno M, Rozendaal L, Meijer CJ, van den Eertwegh AJ, Scheper RJ, von Blomberg ME, Bontkes HJ: CD4(+)CD25hi regulatory T-cell frequency correlates with persistence of human papillomavirus type 16 and T helper cell responses in patients with cervical intraepithelial neoplasia. *Int J Cancer* 2007; 121:1749–1755.

21 Nakamura T, Shima T, Saeki A, Hidaka T, Nakashima A, Takikawa O, Saito S: Expression of indoleamine 2, 3-dioxygenase and the recruitment of Foxp3-expressing regulatory T cells in the development and progression of uterine cervical cancer. *Cancer Sci* 2007; 98:874–881.

22 Gravitt PE, Peyton CL, Alessi TQ, Wheeler CM, Coutlee F, Hildesheim A, Schiffman MH, Scott DR, Apple RJ: Improved amplification of genital human papillomaviruses. *J Clin Microbiol* 2000; 38:357–361.

23 Bosch FX, Sanjose S: Human papillomavirus and cervical cancer – burden and assessment of causality. *J Natl Cancer Inst Monogr* 2003; 31:3–13.

24 Baecher-Allan C, Brown JA, Freeman GJ, Hafler DA: CD4 +CD25high regulatory cells in human peripheral blood. *J Immunol* 2001; 167:1245–1253.

25 Shen T, Zheng J, Liang H, Xu C, Chen X, Zhang T, Xu Q, Lu F: Characteristics and PD-1 expression of peripheral CD4 +CD127loCD25hiFoxP3+ Treg cells in chronic HCV infected-patients. *Virol J* 2011; 8:279–287.

26 zur Hausen H: Papillomavirus and cancer: from basic studies to clinical application. *Nat Rev Cancer* 2002; 2:342–350.

27 Scott ME, Ma Y, Kuzmich L, Moscicki AB: Diminished IFN-gamma and IL-10 and elevated Foxp3 mRNA expression in the cervix are associated with CIN 2 or 3. *Int J Cancer* 2009; 124:1379–1383.

28 El-Sherif AM, Seth R, Tighe PJ, Jenkins D: Decreased synthesis and expression of TGF-beta1, beta2, and beta3 in epithelium of HPV 16-positive cervical precancer: a study by microdissection, quantitative RT-PCR, and immunocytochemistry. *J Pathol* 2000; 192:494–501.

29 Xu XC, Mitchell MF, Silva E, Jetten A, Lotan R: Decreased expression of retinoic acid receptors, transforming growth factor beta, involucrin, and cornifin in cervical intraepithelial neoplasia. *Clin Cancer Res* 1999; 5:1503–1508.

30 Arruvito L, Sanz M, Banham AH, Fainboim L: Expansion of CD4 +CD25+ and FOXP3+ regulatory T cells during the follicular phase of the menstrual cycle: implications for human reproduction. *J Immunol* 2007; 178:2572–2578.

31 Weinberg A, Enomoto L, Marcus R, Canniff J: Effect of menstrual cycle variation in female sex hormones on cellular immunity and regulation. *J Reprod Immunol* 2011; 89:70–77.

32 Brandsma CA, Hylkema MN, Geerlings M, van Geffen WH, Postma DS, Timens W, Kerstjens HA: Increased levels of (class switched) memory B cells in peripheral blood of current smokers. *Respir Res* 2009; 10:108.

33 Barceló B, Pons J, Ferrer JM, Sauleda J, Fuster A, Agustí AG: Phenotypic characterisation of T-lymphocytes in COPD: abnormal CD4+CD25+ regulatory T-lymphocyte response to tobacco smoking. *Eur Respir J* 2008; 31:555–562.

34 Vargas-Rojas MI, Ramírez-Venegas A, Limón-Camacho L, Ochoa L, Hernández-Zenteno R, Sansores RH: Increase of Th17 cells in peripheral blood of patients with chronic obstructive pulmonary disease. *Respir Med* 2011; 105:1648–1654.

OPEN ACCESS Freely available online

PLOS ONE

Effect of Maraviroc Intensification on HIV-1-Specific T Cell Immunity in Recently HIV-1-Infected Individuals

Ai Kawana-Tachikawa[1,2], Josep M. Llibre[3], Isabel Bravo[3], Roser Escrig[3], Beatriz Mothe[1,3,4], Jordi Puig[3], Maria C. Puertas[1], Javier Martinez-Picado[1,4,5], Julia Blanco[1,4], Christian Manzardo[6], Jose M. Miro[6], Aikichi Iwamoto[2], Anton L. Pozniak[7], Jose M. Gatell[6], Bonaventura Clotet[1,3,4], Christian Brander[1,4,5]*, the MARAVIBOOST investigators[¶]

1 Irsicaixa AIDS Research Institute – HIVACAT, Autonomous University of Barcelona, Badalona, Spain, **2** Division of Infectious Diseases, Advanced Clinical Research Center, The Institute of Medical Science, The University of Tokyo, Tokyo, Japan, **3** Lluita contra la SIDA Foundation, HIV Unit, University Hospital Germans Trias i Pujol, Badalona, UAB, Badalona, Spain, **4** University of Vic, Vic, Spain, **5** Institució Catalana de Recerca i Estudis Avancats (ICREA), Barcelona, Spain, **6** Hospital Clínic-IDIBAPS, University of Barcelona, Barcelona, Spain, **7** HIV/GUM Department, Chelsea and Westminster Hospital, London, United Kingdom

Abstract

Background: The effect of maraviroc on the maintenance and the function of HIV-1-specific T cell responses remains unknown.

Methods: Subjects recently infected with HIV-1 were randomized to receive anti-retroviral treatment with or without maraviroc intensification for 48 weeks, and were monitored up to week 60. PBMC and *in vitro*-expanded T cells were tested for responses to the entire HIV proteome by ELISpot analyses. Intracellular cytokine staining assays were conducted to monitor the (poly)-functionality of HIV-1-specific T cells. Analyses were performed at baseline and week 24 after treatment start, and at week 60 (3 months after maraviroc discontinuation).

Results: Maraviroc intensification was associated with a slower decay of virus-specific T cell responses over time compared to the non-intensified regimen in both direct *ex-vivo* as well as *in in-vitro* expanded cells. The effector function profiles of virus-specific $CD8^+$ T cells were indistinguishable between the two arms and did not change over time between the groups.

Conclusions: Maraviroc did not negatively impact any of the measured parameters, but was rather associated with a prolonged maintenance of HIV-1-specific T cell responses. Maraviroc, in addition to its original effect as viral entry inhibitor, may provide an additional benefit on the maintenance of virus-specific T cells which may be especially important for future viral eradication strategies.

Citation: Kawana-Tachikawa A, Llibre JM, Bravo I, Escrig R, Mothe B, et al. (2014) Effect of Maraviroc Intensification on HIV-1-Specific T Cell Immunity in Recently HIV-1-Infected Individuals. PLoS ONE 9(1): e87334. doi:10.1371/journal.pone.0087334

Editor: Derya Unutmaz, New York University, United States of America

Received September 27, 2013; **Accepted** December 19, 2013; **Published** January 27, 2014

Funding: This work was funded by HIVACAT, the Catalan program for the development of therapeutic and preventive HIV vaccines, the European AIDS Treatment Network (NEAT – FP6, contract LSHP-CT- 2006-037570) and Pfizer Inc, and an unrestricted grant from ViiV to support the sub-study to the original Maraviboost clinical phase III trial, which was also sponsored by ViiV. The Hospital Clinic-IDIBAPS cohort was supported in part by the "Ministerio de Sanidad y Consumo, Instituto de Salud Carlos III, Madrid (Spain)," Spanish Network for AIDS Research (RIS; ISCIII-RETIC RD06/006). A.K-T was funded by the Japan Society for the Promotion of Science for the "Institutional Program for Young Researcher Overseas Visits." The funders had no role in study design, data collection and analysis, decision to publish, or preparation of the manuscript.

Competing Interests: *This work was partly funded by Pfizer Inc and ViiV Healthcare. This does not alter the authors' adherence to all the PLOS ONE policies on sharing data and materials.*

* E-mail: cbrander@irsicaixa.es

¶ Membership of the MARAVIBOOST investigators is provided in the Acknowledgments.

Introduction

Maraviroc is an antiretroviral agent that blocks HIV-1 entry by binding the virus' coreceptor CCR5. Given its molecular target, maraviroc treatment may modulate the natural expression and function of CCR5, and negatively affect chemotaxis and effector function of Th1-type $CD4^+$ T cell and memory $CD8^+$ T cells. Maraviroc may have additional immunomodulatory effects by blocking the binding of the natural ligands of CCR5 (MIP-1α, MIP-1β and, RANTES), yet little data exist on how maraviroc may interfere with the cellular host immunity, especially the one directed against HIV-1.

While CCR5 deficiency (in the form of a 32 base-pair homozygous deletion) can mediate resistance to HIV-1 infection [1–3], it also has the potential to impair control of other viral infections, such as West Nile virus (WNV), both in mouse and humans [4,5]. In particular, murine T cells lacking CCR5 expression have been shown to secrete lower amounts of IL-2 compared to $CCR5^+$ T cells, and a similar phenotype has been observed in T cells from humans expressing the CCR5-:32 mutation [6]. Furthermore, $CD8^+$ T cell exhaustion during chronic Lymphocytic choriomeningitis virus (LCMV) infection is more severe in the absence of RANTES, one of the natural CCR5 ligands [7]. Thus, although CCR5-:32 homozygosity does not

seem to negatively affect humans, blocking its function by agents like maraviroc may negatively affect immune responses, including T cell responses to HIV-1.

In previous clinical trials, treatment with maraviroc has been shown to result in more extensive increases in CD4 counts in treatment-naïve and -experienced subjects, though the mechanisms involved remain unknown [8–11]. In addition, some studies have indicated that adding maraviroc to suppressive combination antiretroviral treatment (cART) reduces markers of immune activation [12–15]. Also, *in vitro* exposure to maraviroc decreases some markers of immune activation on T lymphocytes [16]. While these findings suggest that maraviroc may have beneficial effects on global host immune status, maraviroc has also been found to increase T cell activation both in gut and peripheral blood [17]. Thus, it is still controversial whether maraviroc has net immunological benefits or disadvantages on host cellular immune responses. In addition, the impact of maraviroc on antigen-specific T cell responses, especially towards HIV-1-derived antigens, has not been assessed, despite its potential implications with regards to immune interventions, particularly therapeutic vaccination in maraviroc treated subjects. To address these issues, we analyzed in a longitudinal study the effects of cART versus maraviroc–intensified cART on the maintenance (breadth, magnitude and specificity) of HIV-1-specific T cell responses, their differentiation potential and their polyfunctionality.

Materials and Methods

Study design

The present study was performed as sub-study of the Maraviboost study (ClinicalTrials.gov Identifier: NCT00808002). The Maraviboost study was a multi-center, randomized, open-label, phase III clinical trial. The main goal of the parental clinical trial was to assess whether intensification with maraviroc in recently HIV-1 infected patients with standard triple therapy could accelerate the decay of the HIV-1 reservoir [18]. Thirty subjects recently infected with CCR5-tropic HIV-1 (subtype B) were recruited and randomized into 2 groups (n = 15 each), one being treated with triple therapy consisting of Raltegravir (RAL) plus Tenofovir (TDF)/Emtricitabine (FTC) alone while the second group received additionally maraviroc (MVC) intensification for the first 48 weeks in the trial. The primary end point of the main study was week 48, but patients were followed until week 72 if possible. Frozen PBMC from pre-defined time points before starting cART (baseline, BL), 24 weeks after study initiation, and 12 weeks after maraviroc discontinuation (week 60), were analyzed in the present study. One patient without maraviroc intensification, who dropped out the study because of adherence problem, was excluded from the analysis. Three patients (01028, 01039, 23012) were lost at week 24 (n = 1) or 36 (n = 2), respectively. All patients received RAL plus TDF/FTC after week 48 except 4 patients (01021, 01031, 01034, 01043), who changed their anti-HIV drug regimen. Of the 29 individuals, peripheral blood mononuclear cells (PBMC) from at least one time point were available for 13 patients with maraviroc intensification (MVC arm) and 14 patients without MVC intensification (Control, CNT arm, Table 1). The study was approved by the ethics committee of Hospital Germans Trias i Pujol, Badalona, Spain. All patients gave their written informed consent before enrolling in the study.

Flow cytometry for T cell phenotype analysis

PBMC were thawed and rested overnight at 37°C in RPMI1640 supplemented with 10% heat-inactivated FCS, 100 U/ml penicillin, 100μg/ml streptomycin, and 2 mM glutamine (R10). The following day, the cells were stained with LIVE/DEAD Fixable Dead Cell Stain Kits (Invitrogen), washed and stained with the following antibodies: anti-CD3-APC-Cy7, anti-CD4-V450, anti-CD8-PE-Cy7, anti-CD45RA-APC (BD Biosience), and anti-CCR7-PE (e-BioScience). The cells were washed and fixed with 1% Formaldehyde in PBS. All data were collected on a BD LSR II flow cytometer (BD Biosience) and analyzed using FlowJo 8.7.7 (TreeStar).

Peptides

A set of 410 overlapping-peptides (OLPs) was used to screen for HIV-specific T-cell responses [19]. The peptides spanned all HIV-1 proteins and were based on the HIV clade B consensus sequence of 2001, available at the Los Alamos National Laboratory HIV immunology database. For ELISpot analyses, peptides were used in a matrix layout of 6–12 peptides per pool for comprehensive screening as previously described [19]. Reconfirmations of all positive wells in the matrix screen were performed the following day on a single-peptide base. For multi-functional analysis by flow cytometry, peptide pools were used that contained peptides spanning either full-length Gag, Protease, RT, IN, gp120, gp41, or Nef. Peptides spanning Tat, Rev, Vif, Vpr, and Vpu were combined into one peptide pool (accessory proteins peptide pool. "Acc").

IFN-γ ELISpot assay using ex-vivo PBMC and in-vitro expanded T cells

Thawed PBMC were rested for 3 hrs at 37°C in R10. If sufficient PBMC were recovered, thawed cells were used directly in IFN-γ ELISpot assays (11 and 7 samples at baseline, 6 and 7 samples at week 24, and 8 and 7 samples at week 60 in the CNT and MVC arm, respectively). In addition, 1×10^6 thawed cells were stimulated with an anti-CD3 monoclonal antibody and cultured for 2–4 weeks in R10 supplemented with 50 U/ml of recombinant IL-2 [20]. Before use in ELISpot assays, the expanded cells were washed twice with R10 and incubated overnight at 37°C in the absence of IL-2. Per well, 75,000–100,000 cells were used and peptides were added as in the direct ex-vivo assay. Thresholds for positive responses were defined as 1) at least five spots (50–66 SFC/10^6 PBMC) per well, 2) as responses exceeding the mean of negative wells plus 3 standard deviation and 3) responses exceeding three times the mean of negative (no peptide) wells; whichever was the highest. For reconfirmation ELISpot, the remaining cells and cells from negative wells from initial matrix screens were recycled as previously described [20].

Flow cytometric analysis of $CD8^+$ T cell function

Thawed PBMC were rested overnight at 37°C in R10. The following day, costimulatory antibodies (anti-CD28 and anti-CD49d at 1μg/ml; BD Biosciences) and monensin (GolgiStop; BD Bioscience) were added, and cells were stimulated with the different peptide pools (5μg/ml per peptide) as indicated. A negative (no peptide) and a positive control (phorbol-12-myristate-13-acetate (PMA at 10 ng/ml and ionomycin, 1μM) were included in each assay. Following incubation for 6 hrs, the cells were washed with PBS containing 1% FCS and the fluorescent reactive dye (Invitrogen) for dead cells was added. Cells were washed again, and stained with anti-CD3-V450, anti-CD8-PerCP, and anti-CD107a-PE (BD BioScience). Following washing, the cells were fixed and permeabilized using Fix & Perm cell permeabilization reagents (Invitrogen). The cells were then stained with anti-MIP-1β-FITC, anti-IL-2-PE-Cy7, anti-IFN-γ-APC (BD Bioscience). Data were collected on a BD LSR II flow cytometer (BD

Table 1. Characteristics of participants.

patient ID	age	Estimated duration from infection	baseline			week24			week60		
			VL	CD4	CD8	VL	CD4	CD8	VL	CD4	CD8
	(year-old)	(months)	(copies/ml)	(cells/μl)	(cells/μl)	(copies/ml)	(cells/μl)	(cells/μl)	(copies/ml)	(cells/μl)	(cells/μl)
Control group (n = 14)											
01022	28	6.2	61,000	606	873	50	843	731	50	741	606
01025	32	5.8	[a]36,000	287	691	[b]50	446	809	50	432	527
01028	26	3.1	490,000	366	1,893	56	518	900	[c]not determined		
01030	21	4.0	19,000	297	1,124	50	435	464	50	650	650
01032	32	4.5	[a]200,000	372	1,830	200	478	956	50	580	825
01036	42	5.1	40,000	273	1,034	50	352	641	50	429	617
01037	40	3.2	[a]26,000	589	1,326	50	533	999	50	556	641
01039	26	8.6	[a]63,000	450	1,125	50	654	1,162	[c]not determined		
01040	50	2.8	1,500,000	379	2,245	[b]230	601	631	50	620	589
01044	35	3.8	[a]540,000	454	1,127	50	962	1,683	50	396	834
23010	26	4.7	[b]1,091	629	1,204	[b]50	624	559	50	649	593
23012	38	4.0	10,738	656	579	50	688	615	[c]not determined		
23013	39	4.1	30,210	492	1,624	94	644	984	50	624	635
23019	32	6.5	8,497	620	1,033	[b]50	688	899	50	543	688
median	32	4.3	38,000	452	1,126	50	613	854	50	580	635
(itnterquartile range)	(26–39)	(3.7–5.9)	(16,935–272,5000)	(349–610)	(993–1,676)	(50–65)	(470–688)	(627–989)	(50–50)	(432–649)	(593–688)
MVC intensified group (n = 13)											
01021	39	5.1	46,000	649	1,750	50	954	1,371	[c]not determined		
01027	32	6.6	120,000	558	888	50	767	684	50	941	811
01034	33	4.6	12,000	310	496	55	285	498	[c]not determined		
01035	35	4.2	320,000	384	1,024	50	706	1,169	50	984	1,312
01041	34	2.0	160,000	619	1,695	50	1,034	853	50	542	383
01042	33	2.3	[a]140,000	280	1,595	50	602	1,228	50	654	782
01043	37	2.3	320,000	617	1,163	50	679	928	[c]not determined		
01045	49	1.1	[a]470,000	639	408	60	1,077	661	50	832	407
23005	28	5.4	5,666	421	666	[b]50	572	717	[b]50	500	521
23007	26	2.2	149,556	641	1,124	50	770	1,183	50	839	896
23011	31	5.8	11,081	454	1,473	[b]50	680	1,214	50	843	1,448
23015	42	8.2	54,216	283	2,384	61	492	1,638	50	743	1,974
23016	35	6.8	51,478	397	719	50	653	642	50	515	480
median	34	4.6	120,000	454	1,124	50	680	928	50	788	797

Table 1. Cont.

patient ID	age	Estimated duration from infection	baseline			week24			week60		
			VL	CD4	CD8	VL	CD4	CD8	VL	CD4	CD8
	(year-old)	(months)	(copies/ml)	(cells/μl)	(cells/μl)	(copies/ml)	(cells/μl)	(cells/μl)	(copies/ml)	(cells/μl)	(cells/μl)
(interquartile range)	(31–38)	(2.3–6.2)	(29,000–240,000)	(347–629)	(693–1,645)	(50–53)	(587–863)	(673–1,221)	(50–50)	(535–868)	(462–1,346)
P value			*0.5547*	*0.6623*	*0.5603*	*0.5925*	*0.1263*	*0.2547*		*0.0378*	*0.6422*

a: data from the closest previous timpoint for VL, CD4, CD8. The gap was 14-35 days.
b: not analyzed in this study because of sample limitation.
c: not determined because of lost patients.
doi:10.1371/journal.pone.0087334.t001

Biosience) and analyzed using FlowJo 8.7.7 (TreeStar). After gating for each effector function, a Boolean gate platform was used to create the full array of possible combinations and SPICE software (version 5.22) was used to analyze the polychromatic flow cytometry data. We applied a threshold for positive responses using negative values distribution after background subtraction (i.e. unstimulated cultures), as previously described [21].

Statistical analyses

Statistical analyses were performed using Graph Pad Prism 5.0. The results are given as medians and interquartile range (IQR) as indicated. Mann-Whitney test and Wilcoxon matched paired test were used for unpaired and paired comparisons, respectively. For multiple comparison analysis, we performed Bonferroni correction. Correlations between *ex-vivo* and *in-vitro* ELISpot data were analyzed by using Spearman's rank correlation coefficient, and linear regression analysis.

Results

Changes in $CD4^+$ and $CD8^+$ T cell count and their differentiation status

HIV-1-specific T cell responses are known to decrease upon cART initiation, although not all responses and specificities may show similar decay kinetics [22,23]. To determine whether maraviroc-intensified cART would lead to an equally rapid or even faster decay of global T cell responses to HIV-1, longitudinal changes in the breadth and magnitude of total HIV-1-specific T cell responses were compared between the maraviroc and control study arms at week 24 and week 60, i.e. 12 weeks after stopping maraviroc intensification. As previously reported, plasma viral load decreased under the limits of detection within the first 4-week cART in most patients [18]. $CD4^+$ T cell counts showed higher increases in the MVC subjects at week 12 and were significantly elevated in the MVC arm at week 60 when compared to the control subjects ($p = 0.0378$, Table 1 and ref [18]). At the same time, the decay in $CD8^+$ T cells was significantly slower in MVC subjects than in the control subjects (Fig. 1A and [18]) To examine whether these effects on $CD4^+$ and $CD8^+$ T cell counts were associated with a modulation of T cell differentiation markers, the expression of CD45RA and CCR7 was assessed over time and compared between the two groups. The data show that the frequency of effector memory (EM, $CD45RA^-/CCR7^-$) $CD8^+$ T cells was significantly decreased in both study arms at week 24 and week 60 compared to baseline, possibly reflecting the strong reduction in viral loads in both arms upon cART initiation (Fig. 1B). No significant changes for any other $CD4^+$ or $CD8^+$ T cell subset was observed, neither over time nor between study arms. These data indicate that maraviroc does not affect T cell differentiation during and after maraviroc intensification and that the different kinetics of $CD4^+$ and $CD8^+$ T cell counts between the arms are not reflected by gross alterations in differentiation markers.

Maraviroc intensification is associated with maintenance of HIV-1-specific T cell responses

To assess whether the effect of maraviroc intensification on cell homeostasis affected the magnitude, breadth and specificity of the HIV-1-specific T cell response, we performed IFN-γ ELISPOT assay on PBMC from individuals in both arms of the study using a 18-mer overlapping peptide (OLP) set covering the full HIV-1 proteome [19]. At baseline, the median magnitude of HIV-1-specific T cell responses in all patients was 2,708 SFC/10^6 PBMC (range 395–13,860), with a median breadth of 6 (range 2–15)

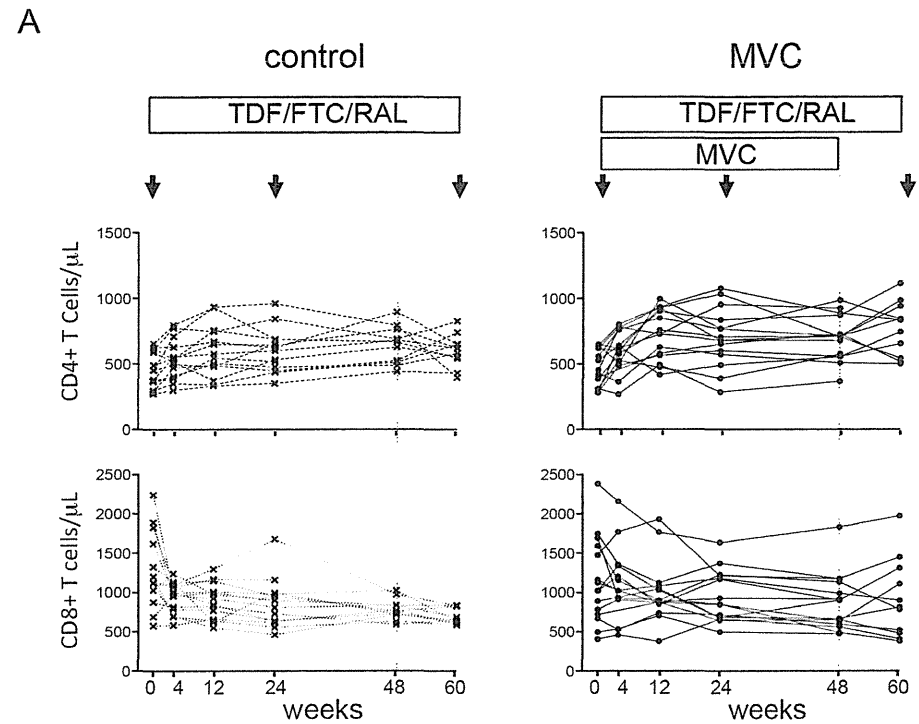
A
control
MVC
TDF/FTC/RAL
TDF/FTC/RAL
MVC
CD4+ T Cells/µL
CD8+ T cells/µL
weeks
weeks

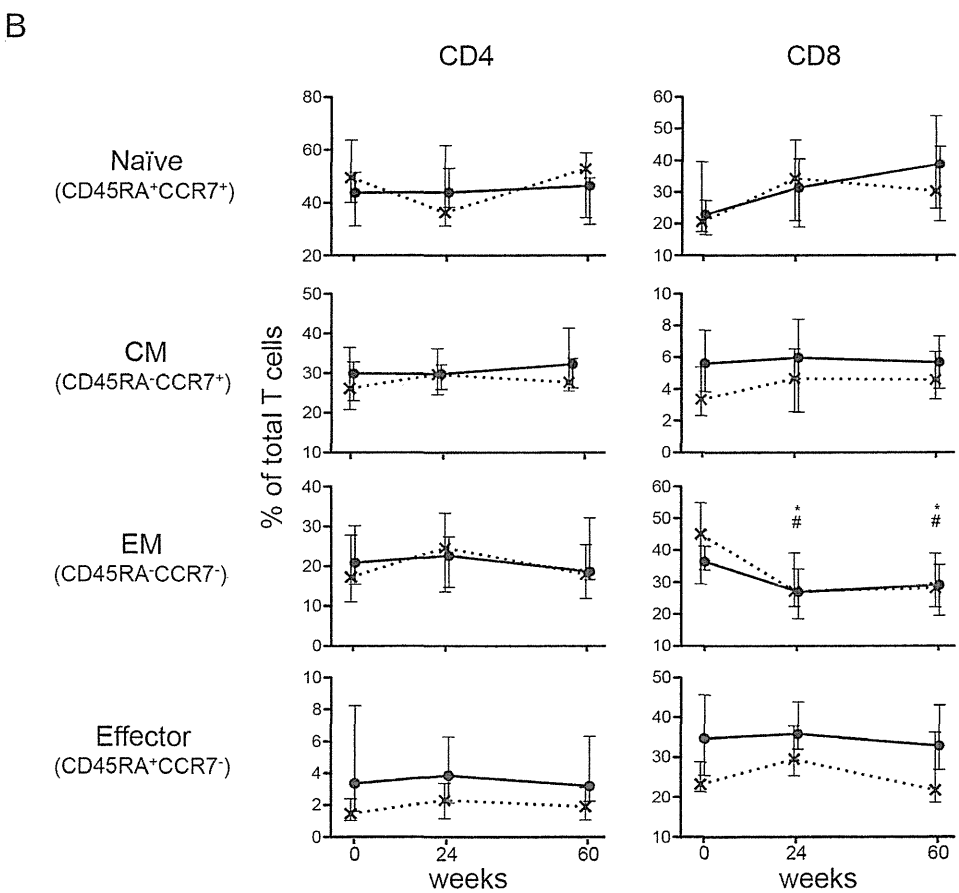
B
CD4
CD8
Naïve
(CD45RA+CCR7+)
CM
(CD45RA-CCR7+)
EM
(CD45RA-CCR7-)
Effector
(CD45RA+CCR7-)
% of total T cells
weeks
weeks

Figure 1. Differentiation status in CD4$^+$ and CD8$^+$ T cells. A. Changes of CD4$^+$ and CD8$^+$ T cell count in each subject. B. The proportion of naïve (CD45RA$^+$/CCR7$^+$), central memory (CM, CD45RA$^-$/CCR7$^+$), effector memory (EM, CD45RA$^-$/CCR7$^-$), and Terminal effector memory (T_{EMRA}, CD45RA$^+$/CCR7$^-$) cells among CD4$^+$ and CD8$^+$ T cells in the control (cross and hatched line) and MVC arm (circle and solid line). The median and interquartile range (vertical line) are shown. Stars (control) and hatches (MVC arm) above the lines indicate significant differences relative to baseline values ($p< 0.05$).
doi:10.1371/journal.pone.0087334.g001

responses per individual (Fig 2, left hand panels). The magnitude and the breadth in this cohort were considerably lower than that of chronically infected patients reported previously but in line with described breadth of responses in early, untreated HIV-1 infection [19,24]. No significant difference was observed in magnitude and breadth of HIV-1-specific response between the arms at any time point (Fig. 2, right panels). When we assessed changes in the virus-specific response in each arm, the magnitude of the HIV-1-specific response in the control arm was significantly reduced by week 24 (median 454 SFC/10^6 PBMC (range 27–7584), $p = 0.0042$) and even more so by week 60 (median 115 SFC/10^6 PBMC (range 0-1,475), $p = 0.0043$, Fig 2A). In contrast, subjects in the MVC arm did not show a significant reduction until week 60 when their median magnitude was still more than 5-fold higher than responses in the control arm (median 691 SFC/10^6 PBMC (range 0–3,535), Fig 2A). Similarly, the breadth of response was reduced over time as well, with significant reductions seen by week 60 in the control arm but not in the maraviroc intensified group (Fig 2B). There was no difference between the arms in regards to protein specificity of the HIV-1-specific CD8$^+$ T cells that remained at 24 and 60 weeks after starting cART (data not shown).

To extend the longitudinal analyses of responses between the intensified and non-intensified arms of the study to additional individuals for whom sample availability was limiting, we performed the same analysis using *in vitro* expanded cells. Aside from including additional individuals into the analyses, this also offered the opportunity to test for potential differences in the proliferative capacities of HIV specific T cells in the two arms. Thawed PBMC were expanded using an anti-CD3 mAb and kept in culture until sufficient cell numbers were reached. The culture time needed between the two study arms was comparable (both arms a median of 19 days), indicating intact proliferative capacities of T cells in maraviroc intensified cART treated individuals. For samples for which direct *ex-vivo* PBMC and *in vitro* expanded cells were tested, the ELISpot results were compared to validate the approach of using *in vitro*, unspecifically expanded cells. Overall, the breadth of responses in expanded cells correlated well with the direct *ex-vivo* results (Fig 3A, $r = 0.78$, $p<0.0001$). The magnitude of responses was generally increased in expanded cells, with later time points (week 24 and 60) showing stronger recovery of responses when compared to unexpanded cells (Fig. 3B). Of note, the correlation between results from direct *ex-vivo* analyses and *in-vitro* stimulated cells became stronger over time ($r = 0.5235$, 0.8455, 0.8720, and $p = 0.0374$, 0.0018, 0.0004 for comparisons at BL, w24, and w60 respectively). No differences were observed in proliferative capacity between the arms These data indicate that in both arms, HIV-1-specific T cell responses showed intact *in-vitro* proliferative capacities after prolonged cART and that in settings with limited sample availability, the *in-vitro* expansion approach produces reliable data [25].

HIV-1-specific T cell responses measured in expanded cells showed a significant decline in their magnitude during first 24 weeks in all subjects together (Fig. 3C, left panel). However, the reduction was generally less than three-fold (median 8,110 SFC/10^6 PBMC in BL and 2,656 SFC/10^6 PBMC in week 24) and thus not as dramatic as in unexpanded cells (median 6.3 fold, 2,708 SFC/10^6 PBMC in BL, and 424 SFC/10^6 PBMC in w24) (Fig. 2A and 3C, left panel). When the longitudinal changes in magnitude and breadth of responses were analyzed for each treatment arm separately, no significant reductions at week 24 and week 60 were noted (Fig 3C, D). However, when *in-vitro* stimulated responses were compared between the two arms, there was a trend that MVC-intensified subjects maintained stronger HIV-1-specific response at week 24 than control individuals (median 1,450 (IQR 277–2,965) in the control arm, 3,957 (1,714–13,018) in MVC, $p = 0.0625$, Fig. 3C, right panel). In addition, the median HIV-specific response was three-fold higher in MVC (median 3,957 (275–4,691)) compared to the control arm (1,114 (2,394–6,882)) until week 60. These data further support the notion that HIV-1-specific T cell responses are maintained for longer at higher levels in subjects with maraviroc intensification compared to individuals receiving non-intensified cART.

Poly-functionality of HIV-1-specific CD8$^+$ T cells is maintained under MVC intensified cART

The ability of HIV-1-specific T-cells to respond to antigenic stimulus with multiple different effector functions has been associated with the relative control of HIV-1 infection [26,27]. Since therapeutic strategies that aim at prolonged treatment interruptions or even viral eradication, will possibly depend on such polyfunctional T cell responses, we assessed the effector functions of HIV-1-specific CD8$^+$ T cells in cART treated subjects with and without maraviroc intensification. To this end, direct *ex-vivo* isolated PBMC were stimulated using peptide pools covering each of the viral proteins and analyzed for the expression of the degranulation marker (CD107a) or the production of intracellular cytokines, including IFN-γ, MIP-1β, and IL-2. The frequency of IFN-γ producing T cell responses correlated well with the data from the *ex-vivo* ELISpot analyses (Fig 4A, $r = 0.8265$, $p<0.0001$). The magnitude of the total HIV-1-specific CD8$^+$ T cell responses with at least one effector function by flow analysis varied widely in baseline samples (0.43% to 16.44% of total CD8$^+$ T cells across arms) and, as expected, was reduced at week 24 and week 60 (Fig. 4B). Although the magnitude of total HIV-specific CD8$^+$ T cells between the arms was comparable at the different time points, a significant reduction in the strength of the ex-vivo response was seen in the control arm but not in MVC arm, as observed in direct *ex vivo* ELISpot analysis (Fig. 1A and 4B). Also, as the reduction in frequency of HIV-specific CD8$^+$ T cell fractions with different cytokine secretion pattern was similar between the two arms, the data indicate that maraviroc intensification does not skew HIV-specific CD8$^+$ T cell function (Fig. 4C). The same was observed when the relative contribution of T cell populations with different numbers of effecter functions to the total HIV-specific CD8 T cell responses was compared between arms and over time (Fig. 4D),in line with previous reports [26,28].

Discussion

Since its development as a HIV entry inhibitor, CCR5 has been used as a target in several clinical studies of HIV infection as well as in other applications, including auto-immune diseases, cancer and transplantation [15,29–34]. Although some results remain still controversial [11–15,17,32] blocking the CCR5 co-receptor is

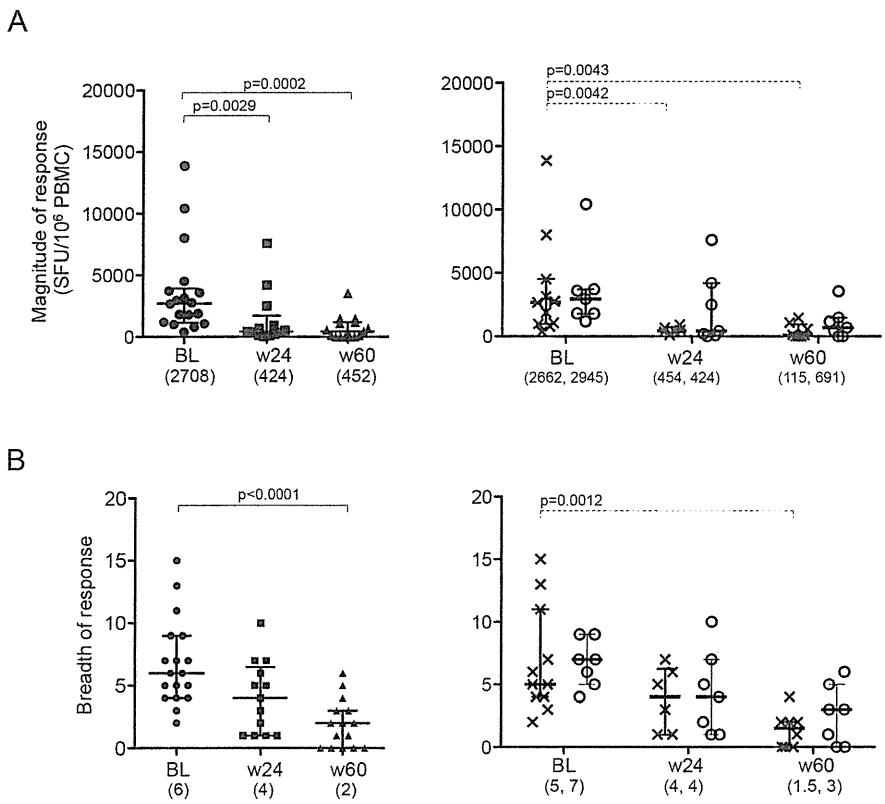

Figure 2. Longitudinal analyses of HIV-1-specific T cell responses in PBMC. The total magnitude (A) and breadth (B) of ELISpot responses at baseline (BL), week 24 (w24) and week 60 (w60) are shown for all subjects together (left panels) and for each study arm separately (right panels, crossed lines for control arm, circles for MVC arm). Horizontal lines represent median values of Spot-forming cells (SFC)/10^6 PBMC and the IQR, respectively. Mann-Whitney test was used in all statistical analysis. Only p values with significance after Bonferroni correction was shown. The numbers in parenthesis below the x-axis represent the median value.
doi:10.1371/journal.pone.0087334.g002

thought to suppress adverse immune activation and inflammation by blocking the chemotactic activity via its inhibition of CCR5-mediated signals. Due to its potential immune-modulatory properties, maraviroc may thus also affect the HIV-specific immune response, not necessarily only in a beneficial manner. While a number of studies have described effects on total T cell counts, $CD4^+$ and $CD8^+$ T cell kinetics and outcome of vaccination to other pathogens [35–39], no study has, to our knowledge, investigated the effect of MVC on the total HIV-1-specific $CD4^+$ and $CD8^+$ T cell response. In the present study, we investigated the effect of maraviroc intensification on HIV-specific T cell responses in primary HIV-1 infected subjects treated with standard cART or maraviroc intensified regimen. Although there was no gross difference in specific T cell subsets, maraviroc intensification showed extended maintenance of stronger HIV-1-specific T cell responses when compared to non-intensified treatment in PBMCs.

Our data in recently infected and early treated individuals showed that maraviroc intensification accelerated recovery of $CD4^+$ T cell counts and maintained higher $CD4^+$ T cell count after its discontinuation (Table 1 and [18]). As $CD4^+$ T cell help is critical for maintenance of memory $CD8^+$ T cells [40], this early increase of $CD4^+$ T cells may also provide the basis for the extended maintenance of virus-specific T cell responses. Alternatively, the maintenance of higher HIV-1-specific T cell responses in maraviroc intensified subjects may be a reflection of a slower reduction in the total $CD8^+$ T cells in the peripheral blood. This would be in line with clinical data showing that maraviroc intensification increase $CD4^+$ T cells faster and reduce $CD8^+$ T cell slower than non-intensified regimen (Fig. 1A and [18]). In addition, others have recently reported that maraviroc intensification increased $CD8^+$ T cell counts in peripheral blood and decreased $CD8^+$ T cells in rectal tissue in chronically HIV-infected subjects on stable cART [17], suggesting a possible *in vivo* redistribution of T cells by maraviroc. However, the relative changes of total $CD8^+$ T cell counts between control arm and intensified group were less pronounced than the extensive changes in HIV-specific $CD8^+$ T cell frequencies, making it unlikely that a MVC-driven redistribution of virus-specific $CD8^+$ T cells would be the sole driving force behind the prolonged maintenance of these cells in the peripheral blood. Maintenance of virus-specific T cells has also be linked to the availability of cognate antigen[22]. As the reduction in virmeia in both arms was comparable, additional mechanisms may be at work in maraviroc-intensified individuals that lead to extended presence of cells. As shown in previous analyses, not all HIV-specific T cell response contract with the same kinetics and some even expand after cART initiation[23]. As there were no differences in the specificity of HIV-specific T cell response between the two arms in the present study, the mechanism for the maintenance of responses in the MVC intensified group remain unclear. One possibility is that the slower CD4 T cell decline in the intensified arm [18], together with a

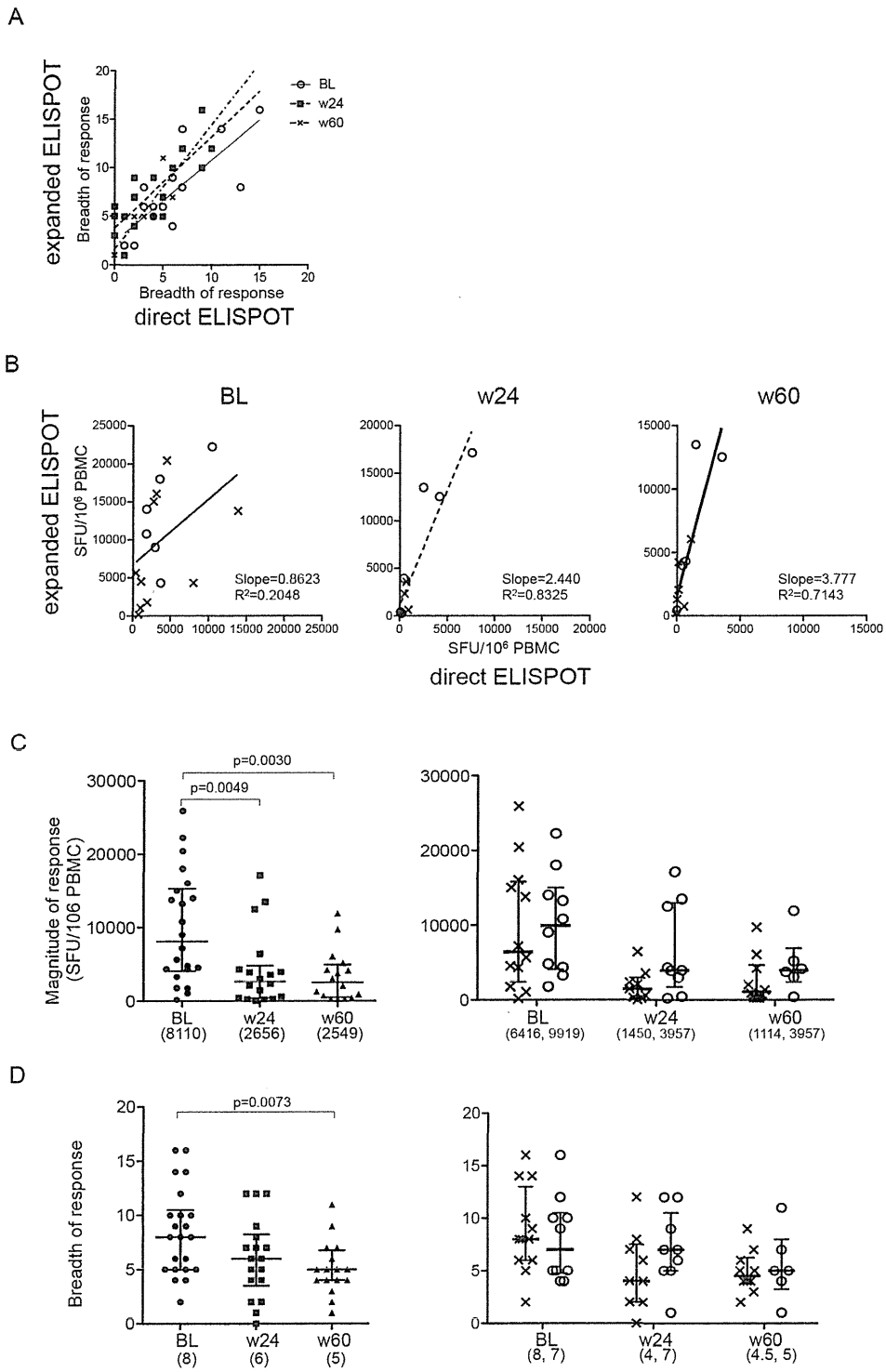

Figure 3. Longitudinal assessment of HIV-specific T cell responses with *in vitro* expanded T cells. A. Relationship of the breadth between responses detected by direct ELISpot and ELISpot using *in vitro* expanded cells. Responses on the x-axes represent the total HIV-1-specific responses in direct ELISpot, and the y-axes indicate total HIV-1-specific responses in expanded ELISpot for samples taken at baseline (circle), week 24 (square), and week 60 (triangle). B. Relationship of the magnitude between direct ELISpot and expanded ELISpot at each time point. cross: control arm, circle: MVC arm. The lines in A and B show linear regression lines. C, D. Changes in magnitude and breadth of total HIV-specific T cell responses in expanded ELISpot are shown as in Figure 2.
doi:10.1371/journal.pone.0087334.g003